A review of reformed methanol-high temperature proton exchange membrane fuel cell systems

Li, Na; Cui, Xiaoti; Zhu, Jimin; Zhou, Mengfan; Liso, Vincenzo; Cinti, Giovanni ; Sahlin, Simon Lennart; Simon Araya, Samuel

Published in:
Renewable and Sustainable Energy Reviews

DOI (link to publication from Publisher):
10.1016/j.rser.2023.113395

Publication date:
2023

Document Version
Publisher's PDF, also known as Version of record

Renewable and Sustainable Energy Reviews 182 (2023) 113395

Contents lists available at ScienceDirect

Renewable and Sustainable Energy Reviews

journal homepage: www.elsevier.com/locate/rser

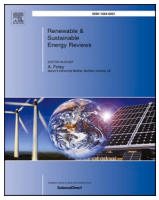

A review of reformed methanol-high temperature proton exchange membrane fuel cell systems

Na Li [a,*], Xiaoti Cui [a], Jimin Zhu [a], Mengfan Zhou [a], Vincenzo Liso [a], Giovanni Cinti [b], Simon Lennart Sahlin [a], Samuel Simon Araya [a]

[a] AAU Energy, Aalborg University, Pontoppidanstræde 111, 9220, Aalborg Øst, Denmark
[b] Department of Engineering, University of Perugia, Via G. Duranti 93, 06125, Perugia, Italy

ARTICLE INFO

Keywords:
Fuel cell
PEM
Methanol steam reforming
System integration
System control
System diagnosis

ABSTRACT

The paper presents a comprehensive review of the current status of integrated high temperature proton exchange membrane fuel cell (HT-PEMFC) and methanol steam reformer (MSR) systems. It highlights the advantages and limitations of the technology and outlines key areas for future improvement. A thorough discussion of novel reformer designs and optimizations aimed at improving the performance of the reformer, as well as different integrated MSR-HT-PEMFC system configurations are provided. The control strategies of the system operation and system diagnosis are also addressed, offering a complete picture of the integrated system design. The review revealed that several processes and components of the system should be improved to facilitate large-scale implementation of the MSR-HT-PEMFC systems. The lengthy system startup is one area that requires improvements. A structural design that is more compact without sacrificing performance is also required, which could possibly be achieved by recovering water from the fuel cell to fulfill MSR's water needs and consequently shrink the fuel tank. Reformer design should account for both heat transfer optimizations and reduced pressure drop to enhance the system's performance. Finally, research must concentrate on membrane materials for HT-PEMFC that can operate in the 200–300 °C temperature range and catalyst materials for more efficient MSR process at lower temperature should be investigated to improve the heat integration and overall system efficiency.

1. Introduction

Consumption of fossil fuels releases carbon dioxide, sulfur dioxide and nitrogen oxides into the atmosphere, causing catastrophic damage to the environment by global warming, climate change, and acid rain. According to the International Energy Agency (IEA) [1], CO_2 emissions from energy sources reached to 31.5 Gt globally even under the effect of Covid-19 lockdowns in 2020 and this value increased to 33.8 Gt in 2022 with the global economic recovery [2]. Also, fossil fuel reserves are depleting fast. Shahriar et al. [3] proposed a new formula to calculate the reserve depletion times of fossil fuels, and their results showed that existing oil and gas reserves will last for approximately 35 and 37 years, respectively. Coal, with a reserve depletion time of 107 years, will be the only remaining fossil fuel after 2042. Therefore, it is urgent to facilitate the fast transitioning from fossil fuels to renewables. It can be seen from Table 1 that renewable energy share increased significantly from 8.7% to 11.2% in a decade, while the fossil fuels share in the total energy consumption remained almost unaltered. Nonetheless, when the fossil fuel demand declined due to the impact of Covid-19 lockdowns, the renewable energy share still increased in 2020 [1,4]. Renewable energy sources are predicted to account for 63% of the total energy supply in 2050 and contribute to greenhouse emission reduction of 94% [5].

Renewable energy sources such as wind and solar energy can be converted into green electricity and be delivered to the power grid for end users. However, despite their great potential, their utilization is difficult due to their fluctuating and intermittent nature. To store energy and balance the power grid, the concept of Power-to-X (PtX) was proposed, in which surplus electric power from renewable energy, typically solar and wind, is converted to hydrogen or other hydrogen-based products through water electrolysis process, where the renewable energies can be stored in hydrogen in the form of chemical energy [6].

Hydrogen, as a clean and renewable energy carrier, has been considered as the most promising substitute to fossil fuels due to the merits of high specific energy density, zero greenhouse gas emission etc. Hydrogen can be stored in gas tank for further use or be used directly in many applications such as transportation or chemical synthesis to produce hydrogen-based products. Another important application of H_2 is

* Corresponding author.
E-mail address: nal@energy.aau.dk (N. Li).

https://doi.org/10.1016/j.rser.2023.113395
Received 11 July 2022; Received in revised form 16 February 2023; Accepted 20 May 2023
Available online 26 May 2023

Nomenclature

Abbreviations

AC	alternating current
AFC	alkaline fuel cell
ANN	artificial neural network
APU	auxiliary power units
AST	accelerated stress test
CFD	computational fluid dynamics
CHP	combined heat and power
CPI	current pulse injection
DC	direct current
ECSA	electrochemical surface area
EIS	electrochemical impedance spectroscopy
FCEVs	fuel cell electric vehicles
FDI	fault detection and isolation
GDL	gas diffusion layer
HER	heat exchanger MSR reformer
HT-PEMFC	high temperature proton exchange membrane fuel cells
IEA	international energy agency
KPI	key performance index
LT-PEMFC	low temperature proton exchange membrane fuel cells
MCFC	molten carbonate fuel cell
MD-WGSR	methanol decomposition-water gas shift
MEAs	membrane electrode assemblies
MeOH	methanol
MFPS	methanol fuel processing system
MSR	methanol steam reforming
MSR-HT-PEMFC	methanol steam reformed HT-PEMFC system
OCV	open circuit voltage
PAFC	phosphoric acid fuel cell
PBI	phosphoric acid doped polybenzimidazole
PEMFC	proton exchange membrane fuel cells
PFSA	perfluorosulfonic acid
PI	proportional integral
Pt	platinum
PtX	power-to-X
SOFC	solid oxide fuel cell
S/C ratio	steam-to-carbon ratio

Parameters

ΔH_{298K}	enthalpy of reaction, $kJ\ mol^{-1}$
F_{MeOH}	flow rate of feed methanol solution, $mol\ s^{-1}$
m_{cat}	weight of catalyst, kg
$\dot{q}_{Burner,air.}$	the volumetric air flow to the burner, $L\ min^{-1}$
$T_{Burner,\ Setpoint}$	reformer setpoint temperature, K
$T_{Reformer,\ Setpoint}$	burner setpoint temperature, K
WHSV	weight hourly space velocity, h^{-1}
λ	stoichiometric ratio

Table 1
Comparison of different energy sources share in the total energy consumption of 2009 and 2019 [4].

	Fossil fuels	Renewables	Non-fossil fuel and non-renewables
2009	80.3%	8.7%	11%
2019	80.2%	11.2%	8.7%

as a fuel for proton exchange membrane fuel cells (PEMFC), which converts the chemical energy in H_2 into electricity. As shown in Table 2, H_2 has high energy density of 143 MJ/kg, but the volume of 1 kg of H_2 is as high as 12.3 m^3 at 25 °C and 1 atm, and the high cost and risk for H_2 storage and transportation make its large-scale applications hindered [7]. Therefore, alternative fuels such as natural gas and alcohols have drawn great attention as they can produce H_2-rich gas through fuel reforming process [8,9], and the generated reformate gas can be fed directly into a high temperature PEMFC (HT-PEMFC) and become easy to handle substitute for pure hydrogen.

The commonly seen fuel reforming processes are steam reforming, autothermal reforming and partial oxidation. Approximate 50% of the fuel is consumed to providing the heat required for partial oxidation and auto-thermal processes, which leads to lower efficiency of the reformer-fuel cell system [10]. For autothermal reforming and partial oxidation reforming process, the H_2 content in the reformate gas is only about 49.12 vol % and 40 vol%, respectively [11]. Therefore, steam methanol reforming stands out due to its higher H_2 yield (70 vol% - 80 vol%) and lower reforming temperature (200 °C – 300 °C) and low CO content (1 vol% - 2 vol%) [7,12,13]. Besides, methanol steam reforming also has the advantages of longer catalyst lifetime and easier fuel flow control compared with the other two reforming processes [14].

Nowadays, over 95% of worldwide hydrogen is produced from a mature process of natural gas steam reforming [15]. However, as shown in Table 2 the operating temperature required for natural gas steam reforming is quite high and natural gas is a fossil fuel. Compared with natural gas and other hydrocarbons, methanol has several advantages [9,16–19]: (1) methanol is in liquid phase at standard atmospheric pressure and temperature with higher volumetric energy density than H_2, and can use the existing petroleum infrastructure with only few modifications; (2) methanol has higher H/C molar ratio of 4:1, leading to higher H_2 content in the reformate gas; (3) methanol steam reforming has lower steam reforming temperature due to the lack of C–C bonds, which makes the reforming process easier; (4) methanol can be produced both from renewable sources such as biomass and or non-renewable energy sources such as natural gas, coal etc. and (5) methanol reformates are sulfur-free and the CO content is low, which can be directly fed into an HT-PEMFC. Therefore, hydrogen rich gas from methanol steam reforming is a promising substitute of H_2 as fuel for high temperature PEMFC. A disadvantage of methanol as an energy carrier is related to health and safety. Methanol is toxic to humans, if ingested or if vapors are inhaled, and its flames are practically invisible in sunlight [20–22]. Proper handling and safe storage are needed.

In recent years, there has been some research investigating methanol reformer integration with HT-PEMFC system (MSR-HT-PEMFC). Tian et al. [23] developed a dynamic model of reformed methanol fuel cell

Table 2
Comparison between hydrogen and other popular hydrogen carriers.

	Hydrogen	Natural gas (CH_4)	Methanol (CH_3OH)	Ethanol (C_2H_5OH)
Energy density (MJ/kg)	143	55	22.5	27
Volume of 1 kg (L)	11200	1.96	1.26	1.27
H/C molar ratio	–	4:1	4:1	3:1
Steam reforming temperature (°C)	–	800–1000	200–300	300–500
Renewability	Renewable	Non-renewable	Renewable	Renewable

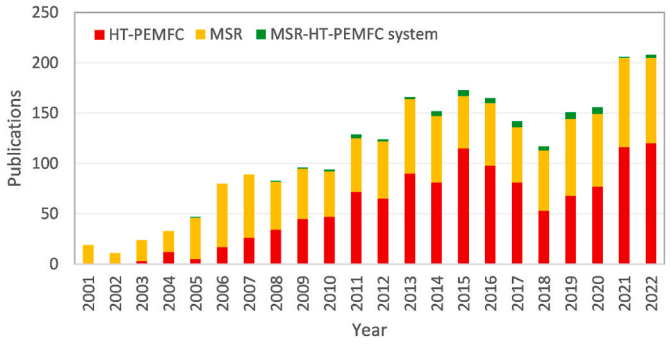

Fig. 1. Trend of yearly publications from 2001 to 2022 regarding HT-PEMFC, MSR and MSR-HT-PEMFC system (the search was made on the Nov 22, 2022 using the Scopus database).

system using Modelica language, where three subsystem models of fuel processor, HT-PEMFC stack and heat recovery were included and verified with experimental data for system analysis and control. Thomas et al. [24] carried out experimental work to investigate the effects of different break-in procedures, including different break-in times and fuel compositions during break-in and found that the effect of break-in on cell performance is negligible but neat hydrogen during break-in can ensure longer durability for the reformed methanol fuel cell system. The effects of catalysts, operating temperature, steam to carbon ratios and other operation parameters on the system efficiency were also studied both in experiments and simulations [18,25–28]. Furthermore, the growing research interest on MSR-HT-PEMFC is confirmed by publication trend over the last 20 years as shown in Fig. 1.

Even though, there are several review articles on HT-PEMFCs and MSRs as separate entities, there is no systematic review in open literature that covers all aspects of MSR-HT-PEMFC systems. This review is therefore devoted to providing systematic information on the MSR-HT-PEMFC systems to both beginning and experienced researchers who are contributing to the development of these systems. The originality of the current work lies in its comprehensive and up-to-date overview of the integrated MSR-HT-PEMFC systems and their configurations, control strategies, diagnostic methods, and key areas for their future improvements. The review summarizes the integration of MSR-HT-PEMFC system which is organized as follows: Section 2 gives a brief introduction to the fundamentals of PEMFC, MSR and their integration. Section 3 reviews typical reformer types and the designs of different system configurations. Section 4 provides the state of the art of optimization and control strategies and diagnostic methods for MSR-HT-PEMFC system. Section 5 presents an overview of the applications of integrated MSR-HT-PEMFC systems. And the current status and prospects of the technology are discussed in Section 6. Finally, Section 7 gives the concluding remarks and the future development trend of this technology.

2. Methanol steam reformer-high Temperature-PEMFC system

A typical MSR-HT-PEMFC system mainly consists of three subsystems: methanol steam reforming subsystem, which usually consists of a steam reformer and a catalytic burner, fuel cell subsystem and heat recovery system.

2.1. PEM fuel cells

Fuel cell is an electrochemical energy conversion device that can convert the chemical energy in the reactants directly into electrical energy. Based on the electrolyte types, fuel cells can be classified into five technologies, namely, proton exchange membrane fuel cell (PEMFC), phosphoric acid fuel cell (PAFC), alkaline fuel cell (AFC), solid oxide fuel cell (SOFC) and molten carbonate fuel cell (MCFC). The main characteristics, operating conditions and efficiencies of the different fuel cell technologies are listed in Table 3. Compared with the other fuel cell types, PEMFC has the advantages of low operating temperature, quick start-up time, high power density, which make it competitive, especially in transportation and portable applications.

2.1.1. The working principle of a PEMFC

A single PEMFC is a sandwich structure consisting of bipolar plates, gas diffusion layers, catalyst layers on both sides and a proton exchange membrane as electrolyte in the middle as shown in Fig. 2. H_2 is fed to the anode and oxidized to produce protons. The protons then transfer from the anode through membrane to the cathode and are reacted with oxygen that is fed to the cathode and with the electrons that are transported through an external circuit to produce water, electricity and heat. The reactions that take place in PEMFC are:

$$\text{Anode}: 2H_2 \rightarrow 4H^+ + 4e^- \quad (1)$$

$$\text{Cathode}: O_2 + 4H^+ + 4e^- \rightarrow 2H_2O \quad (2)$$

$$\text{Overall reaction}: 2H_2 + O_2 \rightarrow 2H_2O \quad (3)$$

2.1.2. Low temperature PEMFC and high temperature PEMFC

As shown in Table 3, the working temperature of PEMFC is below 100 °C (also called low temperature PEMFC). The membrane materials used in low temperature PEMFC (LT-PEMFC) are Perfluorosulfonic acid (PFSA) membranes, which are represented by Nafion® membranes. This

Table 3
Comparison of different fuel cell technologies [29–31].

Fuel cell type	PEMFC	PAFC	AFC	SOFC	MCFC
Electrolyte	Perfluorosulfonic acid (PFSA)	Liquid phosphoric acid	Aqueous alkaline solution (KOH)	Solid oxide or ceramic	Molten carbonate salt
Charge carrier	H^+	H^+	OH^-	O^{2-}	CO_3^{2-}
Fuel	H_2,	H_2	H_2	H_2, CH_4, biogas	H_2, CO, CH_4, C_3H_8
Operating temperature (°C)	50–80	150–210	Room temperature - 250	600–1000	600–700
Electrical efficiency (%)	40–70	45–50	Up to 70	45–60	40–60
Advantages	Low operating temperature, low noise, quick start-up, fast response, high power density	High tolerance to fuel impurities, suitable for CHP	Fast electrooxidation reaction, high efficiency	High CHP efficiency, long-term stability, fuel flexibility, low emissions, low cost	Fuel flexibility, suitable for CHP, high efficiency
Disadvantages	High catalysts cost, low tolerance to impurities, poor heat and water management	Expensive catalysts, long start-up time, sulfur sensitivity	Prone to CO_2 poisoning, high cost for fuel purification	Longer start-up times, mechanical and chemical compatibility issues	Slow start up, high cell component degradation, high performance degradation
Applications	Transportation, distributed/ stationary and portable power generation, backup power,	Stationary power generation, vehicles	Military, space shuttle	Stationary power generation, CHP system, auxiliary power	Large, stationary power plants

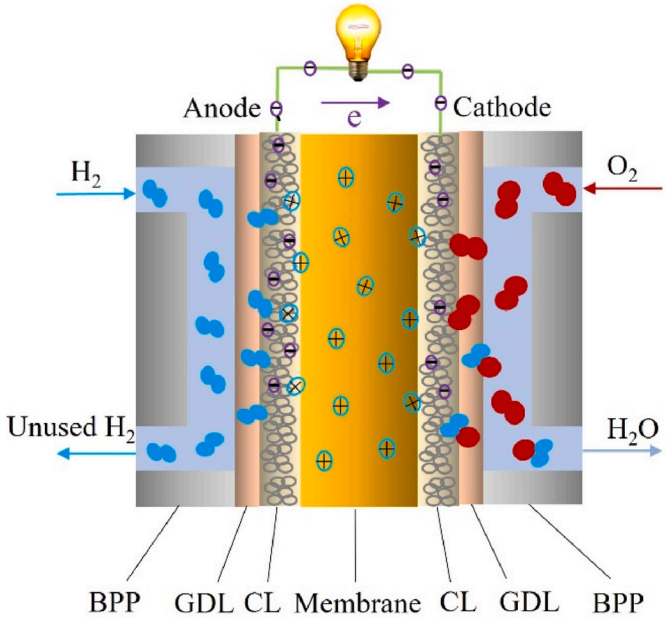

Fig. 2. Schematic of PEMFC.

type of membrane should be maintained at the proper water content and operating temperature to ensure efficient transfer of protons and to avoid membrane dehydration or flooding [32,33]. For instance, high temperature operation (above 80 °C) will lead to the membrane dry up, while low temperature does not benefit the reaction kinetics [33,34]. These water and heat management issues can limit the operational flexibility of LT-PEMFC systems. Furthermore, LT- PEMFCs can only use pure H_2 as fuel because the Pt-based catalysts are more sensitive to impurities that can cause poisoning at low temperatures [35,36]. However, storage and transportation of H_2 have always been obstacles that significantly hinder the large-scale commercial deployment of this technology [31,32].

Thanks to advancements in membrane and catalyst materials, it was made possible to operate PEMFCs at higher temperatures of 120 °C – 200 °C using phosphoric acid-doped polybenzimidazole (PBI) membranes. In these membranes, the phosphoric acid acts as the proton carrier, eliminating the need for membrane hydration and simplifying water and heat management [37,38]. The main advantage of high temperature operation, other than higher quality heat, easier heat rejection and easier water management, is the fact that the CO adsorption on Pt-based catalyst surface is disfavored at high temperature condition, leading to enhanced tolerance to CO and other impurities [39–41]. It has been reported that 10 ppm– 20 ppm CO in feed can cause significant performance decrease for low temperature PEMFC [42]. On the other hand, for HT-PEMFC the CO tolerance can reach up to 1000 ppm when operated at 130 °C [43], 10000 ppm when operated at 150 °C [39] and 30000 ppm when the operating temperature is higher than 160 °C without significant decrease in performance [44]. This high tolerance of HT-PEMFCs to CO poisoning expands the fuel flexibility of the system, allowing reformate gases from hydrocarbons and alcohols, such as methanol to be directly used without any pre-purification. Extensive research has been conducted on the performance evaluation of HT-PEMFCs using both experiments and modeling, as summarized in Table 4. It can be seen that the operating parameters such as temperature, stoichiometry, current density, etc. have a significant effect on the performance of HT-PEMFCs. In recent years, research interests in the system-level performance of HT-PEMFCs using reformates as fuel have increased, and the reported performances have been remarkable [28,45] as shown in Table 4.

2.2. Methanol steam reforming

MSR is an endothermic process, where methanol and water react at high temperature to produce hydrogen-rich gas mixture, known as reformate gas. The reaction mechanism of this process is complex since different reaction pathways could occur in the process as listed in Table 5. There are four types of MSR process, including: (1) photocatalytic MSR, (2) aqueous-phase reforming of methanol, (3) high temperature MSR, (4) thermal catalytic MSR, which are explained in Refs. [57,58].

This study focuses on thermal catalytic MSR, where three reactions are considered, including one main reaction and two side reactions:

$$\text{Main MSR reaction}: CH_3OH + H_2O \rightarrow CO_2 + 3H_2 \Delta H_{298K} = 49.37\ kJ\ mol^{-1} \quad (4)$$

Side reactions:

$$\text{Methanol decomposition}: CH_3OH \rightarrow CO + 2H_2 \Delta H_{298K} = 90.47\ kJ\ mol^{-1} \quad (5)$$

$$\text{water} - \text{gas shift reaction}: CO + H_2O \rightarrow CO_2 + H_2 \Delta H_{298K} = -41.10\ kJ\ mol^{-1} \quad (6)$$

The catalysts for MSR mainly include copper-based and group VIII metal-based catalysts, with the former being the most commonly used in industrial applications. Recent developments of MSR catalysts can be found in Refs. [59,60]. Typically, a mixture of methanol and steam (water) is reacted on a commercial $Cu/ZnO/Al_2O_3$ catalyst bed at a temperature range of 200 °C – 300 °C and steam-to-carbon ratio (S/C) between 1 and 2, to produce a reformate gas composed of H_2, CO_2, CO and unreacted CH_3OH and H_2O. The H_2 content of the reformate gas can reach up to 75% at the reforming temperature of 250 °C – 300 °C, with CO concentration lower than 1 vol%, and can be used as anode feed for high temperature PEMFCs without purification [61–64]. Therefore, methanol reforming system is highly suitable for integration with a high temperature PEMFC system.

2.3. Reformer- fuel cell system

A reference MSR-HT-PEMFC system (H3-350), developed by Serenergy (now Advent Technologies) in Denmark, is usually used in many related studies [7,41,64–68]. As shown in Fig. 3, the system is made up of: a burner providing sufficient heat to keep the reformer at working temperature; an evaporator, where the phase transition of water and methanol mixture from liquid to gas occurs; a reformer, where the MSR reaction occurs and a HT-PEMFC stack, which uses the reformate gas generated from the reformer as fuel to produce electricity. In such a system, no additional CO removal component is required as HT-PEMFC has high tolerance to the impurities in the reformate gas, such as CO and unconverted methanol. Moreover, the unreacted hydrogen is fed to the burner and the excess heat released by the HT-PEMFC can be used in the evaporator to achieve effective utilization of both fuel and heat.

3. The design and integration of MSR-HT-PEMFC system

The working temperature ranges of MSR reformer and HT-PEMFC are different, which can be a challenge for thermal integration of the system. Therefore, research has been carried out on the thermal integration of HT-PEMFC with MSR system to improve the performance and energy efficiency of the system. The waste heat released from HT-PEMFC, which is around 50% of the input chemical energy, can be used to meet heat demand of fuel vaporization and MSR reaction for the methanol reformer subsystem [70].

Table 4
Literature review of HT-PEMFC performance evaluation.

Publication year	Temperature (°C)	λ_{H2}	λ_{Air}	Current density (A cm^{-2})	Test mode	Main Results	Ref.
2012	160	2	2	0.3, 0.4, 0.6	3D modeling (CFD)	In terms of current density homogenization, anode and cathode in counter-flow with cooling and anode in co-flow is the most preferred arrangement.	[46]
2014	140–180	H_2 - 90% methanol conversion	4		Experiment	Degradation rate of −55 mV/h was obtained after 100 h test at 90% methanol conversion.	[18]
2015	160	1.35	2–3			A system efficiency of 27–30% was obtained.	[47]
2015	150–60	1,2	2.2	0.2	Experiment and simulation	The degradation rate for start-stop cycling test was 17.2 μV h^{-1} and 15.3 μV h^{-1} for constant load operation.	[48]
2016	160	2, 4, 6	2	0.2, 0.4, 0.6	Experiment	Increasing current density (increasing water flux) lead to the equivalent crossover current increases.	[49]
2016	150–175	1.25–1.4	2–4	0.09–0.18	Model and experiment	Higher operating temperature (175 °C) improved cell performance, model and experiment data fit well.	[50]
2017	160	1.8 1.8 1.8	2.5 O_2 (same flow of air) H_2 (30 Nml min^{-1})	0.3	Experiment	In Nyquist plots, oxygen reduction reaction contributed mainly at low and intermediate frequency region, high frequency region attributed to anode and proton conduction mechanisms.	[51]
2017	160–200	1.2	2	0.1–1.2	Experiment/3D model (Fluent)	The modeling predictions fits the experimental values well.	[52]
2017	167	1.2 (with reformate composition content changes)	2.5	0.03–0.6	Experiment	CO contamination resulted in an increase in activation losses, methanol pronounced increase in ohmic losses.	[44]
2017	160–200	1.2	2	0.2		MSR-C/HT-PEMFC system obtained remarkable performance with a degradation rate of 138 μV h^{-1} after 700 h test at 180 °C	[53]
2017	160, 180	1.2	4	0.2, 0.4, 0.6	Experiment	Cell performance degradation with reformate as feed was not affected by operating temperature (−39 μV h^{-1} at 160 and -37 μV h^{-1} at 180).	[45]
2018	160	1.3	2	0.1, 0.3, 0.5	Experiment and CFD modeling	The reported model can evaluate the global operational parameters. The results obtained well fitted the theoretical expectations.	[54]
2019	160	1.2	2	3 min at 0.5 V and 3 min at 0.9 V	AST Experiment with different flow channel design	Pt oxidation and reduction take place during each cycle resulting in ECSA loss. Flow field design of cathode side has a strong influence on degradation behavior associated with potential cycling.	[55]
2020	120, 150, 180				Dymola Model	Basic system analysis and design model for RMFC.	[56]

Table 5
Different reaction pathways of MSR [58].

Reaction pathways	Reactions
Methanol decomposition-water gas shift (MD-WGSR)	$CH_3OH \rightarrow CO + 2H_2$ $CO + H_2O \rightarrow CO_2 + H_2$
One-step MSR	$CH_3OH + H_2O \rightarrow CO_2 + 3H_2$
Reverse water gas shift	$CO_2 + H_2 \rightarrow CO + H_2O$
Methyl formate intermediate pathway	$2CH_3OH \rightarrow HCOOCH_3 + 2H_2$ $HCOOCH_3 + H_2O \rightarrow CH_3OH + HCOOH$ $HCOOH \rightarrow CO_2 + H_2$

3.1. Reformer design

Methanol steam reformers, where the methanol steam reaction happens, play a significant role in the MSR-HT-PEMFC system. The performance evaluation and optimization have been carried out extensively as summarized in Table 6. The operating parameters can affect the reformer performance significantly. Besides, the reformer and catalysts design can directly determine the conversion efficiency of methanol and CO concentration in the reformates, which will affect the system efficiency and lifetime of the fuel cell. The development of catalyst materials for methanol conversion reaction and studies on the improvement of the activity and stability of the catalysts have been carried out and summarized in Refs. [26,57,71–73]. However, reviews on the design and optimization of the MSR reformers to improve the methanol conversion efficiency and the performance of the system are scarce.

The design of the reformers should target high methanol conversion efficiency, low by-product content (mainly CO content in the reformate gas), long service life of the components and easy heat integration. Besides, low cost, small weight and volume of the reformer, easy operation and short start-up time should also be considered as important factors to evaluate the MSR performance. To improve the efficiency of the integrated system, different MSR reformer designs have been proposed for use with HT-PEMFCs. Optimization parameters in these MSR designs mainly include more uniform flow distribution of gases and lower pressure drop in the reformer, which can contribute to improved methanol conversion efficiency and lower CO concentration in the reformate gases.

3.1.1. Packed bed MSR

Packed bed reformers are conventionally used for methanol steam reforming, where pellets or cylindrical catalyst particles are packed on the reactor bed. A pump is usually required to provide the driving force for the reactants and products through the reactor. This kind of reformers have the advantages of moderate cost, easy operation and better catalyst availability and reproducibility, but they also suffer from issues of heat transfer limitation and large axial and radial temperature gradients along the bed, which could lead to the catalyst sintering, and thus, large pressure drop along the catalyst bed [85,86].

In order to optimize the heat transfer process and lower the pressure drop in the catalyst bed in packed bed reformers, both experimental and modeling work have been widely carried out [12,61,78–80]. Ribeirinha

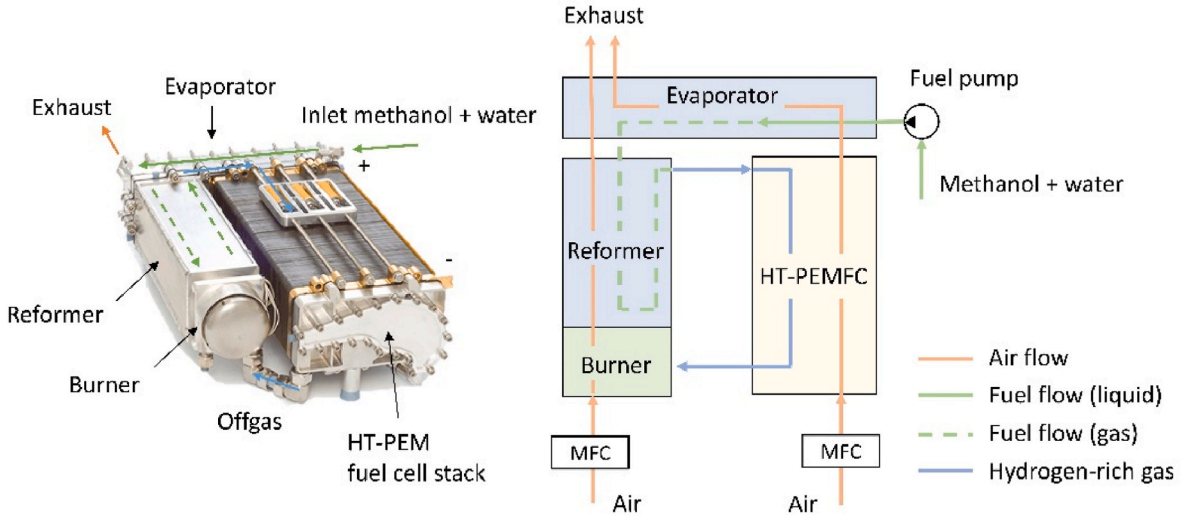

Fig. 3. Scheme (left) and concept drawing of the commercial H3-350 MSR-HT-PEMFC system (right) (reproduced from Ref. [69]).

Table 6
Summarization of methanol steam reformer performance evaluation.

Publication year	Temperature (°C)	Space-to-time ratio	S/C ratio	Test mode	Main Results	Ref.
2012	240-300 in positive steps of 20	200–400 ml/h in positive steps of 100 ml/h	1.5	Experiment	The gas quality of reformate fits HTPEM grade quality requirements. Increasing temperatures increase the CO content of the reformate gas and decreases the methanol slip.	[64]
2015	260	6500 ml/h	1.5	Experiment and modeling	Startup time of the reformer in about 45 min was obtained	[47]
2016	325–375	7.5 and 60 $mmol_{MeOH}/min\ g_{cat}$	1.5	Experiment	High methanol conversion can be achieved with high temperature with very low CO content (<1.5%) in the outlet stream.	[63]
2016	220–320	methanol supply flow rate was set at 15.8 g/min	1.2, 1.4	Experiment	The reformer heat exchanger engine speed increasing can lead to decreased H_2 molar flow rate and methanol conversion efficiency.	[74]
2017	170–200	100-2100 (m_{cat}/F_{MeOH} (kg mol^{-1} s))	1.5	Experiment/3D model (Fluent)	The modeling predictions fits the experimental values well.	[75]
2017	150	0.01 ml/h to 0.5 ml/h	1.0–1.6	3D CFD model	Both methanol conversion and hydrogen molar flow rate increase with increasing S/C ratio and reaches its maximum (optimum) value at 1.4.	[76]
2017	200–240	0.1–1 m/s	1–1.6	Modeling	Methanol conversion decreased with inlet reactant velocity and increased with water methanol molar ratio. CO content increased with temperature but decreased with inlet velocity and water methanol molar ratio.	[77]
2018	210–290	1.5–3.5 L/min	0.5–2.0	CFD modeling	The methanol conversion rate increased with temperature and S/C ratio but decreased with the flow rates of the feedstocks.	[78]
2019	250–350	0.1 g/s	1–1.4	Experiment and modeling	Optimum of operating temperature of 200 °C, S/C ratio of 1.4) and operating capacity of one tubular reactor array were discovered.	[61]
2019	25–600		0–7	Modeling (Aspen Plus)	The optimum MSR temperature of 246 °C, pressure of 1 atm and S/C ratio of 5.6 were proposed	[79]
2020	240–260	2-10 (m_{cat}/F_{MeOH} (kg mol^{-1} s))	1	CFD model	Optimization of operation parameters and reformer design.	[80]
2020	100–400		1–3	Modeling (Aspen Plus)	The optimum values of the temperature, S/C ratio and pressure to produce reformate were identified to be 200–300 °C,1.6–2.0 and 1.0 atm, respectively.	[81]
2020	225–325	0.4–6.7 h^{-1}	1.1–1.5	CFD simulation and experiment	A novel multichannel micro packed bed reactor was proposed. Increase of the S/C and T, as well as decrease of the WHSV and catalyst particle size, both enhance the methanol conversion.	[82]
2020	225–325	0.67–5.36 h^{-1}	1–1.5	3D modeling	The operating temperature plays a more important role than S/C and WHSV. And the operating conditions of T of 275 °C, S/C of 1.3 and WHSV of 0.67 h^{-1} are recommended for the novel multichannel reactor fully packed with catalyst.	[83]
2020	250	Methanol flow rate of 2.31 g/min	1.3	Steady-state test	The MFPS can produces a reformate flow of 3.32 L/min for hydrogen production and total energy efficiency is about 74.2% with low CO content.	[84]
	20–240	Methanol flow rate of 1.99, 2.62, and 3.12 g/min, air flow of 20.2 L/min		Startup test	Startup time was about 15.3 min for the methanol flow rates of 2.62 and 3.12 g/min, 17.8 min for the methanol flow rates of 1.99.	
2021	200–280	0.4–1.2 h^{-1} (methanol liquid hourly space velocity)	1.0–1.8	Experiment	Better performance was achieved at operation condition of 260 °C.	[12]
2021	170–200	650-2000 (m_{cat}/F_{MeOH} (kg mol^{-1} s))	1.5	Experiment	An expansion vessel between the HPLC pump and the evaporator reduced the flow rate oscillations and increased the methanol conversion from 93% to 96%	[53]

et al. [87] manufactured and analyzed three cellular reformers with different designs, including multi-channel, radial and tubular in their study and found that the multi-channel design was the best among the three for the thermal integration as it provides higher methanol conversion rate, uniform temperature and flow distribution and lower pressure drop. Harvey Wang et al. [88] evaluated three different reactor designs with multiple columned-catalyst bed, which were made of different structures and materials that operated at the same condition. The results showed that cylindrical and rectangular reactor shapes showed higher thermal efficiency, smaller temperature differential and shorter start up time than the traditional tubular reactor. Besides, the reformer made of aluminum alloy of Al-6061 with a flameless combustion heating device exhibited effective methanol conversion performance. Feng Ji et al. [89] proposed a single channel serpentine packed bed reformer design with optimized bed diameter of 5 mm incorporated in an internal methanol reforming fuel cell system. It was found that this design led to more uniform temperature distribution as well as lower bed pressure drop, achieving the reported highest power density of 0.45 W cm^{-2}– 0.55 W cm^{-2} with only one-third the catalyst loading used by A. Mendes [70]. Prashant Nehe et al. [90] developed an annular packed bed reformer configuration, where a reformer and vaporizer were integrated together. A rod-type heater was inserted in the center of the reformer to provide heat for the endothermic MSR. Compared with the externally heated reformer, this internal heating design increased the methanol conversion efficiency by 3% – 4% due to the optimized temperature gradient along the radius of the pecked-bed reformer. Perng et al. [91]established a 3D computational fluid dynamics (CFD) model where a diffuser was installed before the catalyst bed in the traditional reformer. They found that the novel design with a diffuser exhibited improved MSR performance and increased net power output of the fuel cell, because the diffuser with suitable angle and length can expand the fuel channel space, which will reduce the fuel velocity and increase the fuel residence time on the catalyst bed. Besides, this novel design avoided large pressure drop and lowered the CO content in the reformates.

Although optimization of different designs on the reformer channels, catalysts, component materials, reformer shapes, etc., have been proposed for packed bed reformer and performance and efficiency have been improved to some extent, these optimizations of the design and configuration often come with higher cost and manufacturing complexity. Besides, the volume and weight of the packed bed reformer should also be considered in the heat-integrated system, especially for portable applications. Multidisciplinary design optimization of packed bed reformer to maximize the methanol conversion rate, heat transfer efficiency, catalyst stability and reaction selectivity are still necessary.

3.1.2. Plate-type MSR

The limitation of heat transfer and large pressure drop in a conventional packed bed reformer promoted the development of plate-type reformers, in which the catalysts are coated on the walls of the reforming channels, forming a wall-coated or suspended catalytic layer configuration. This structure separates the entire channel into two different domains of catalyst-packed domain and the free-fluid domain [92]. Compared to the packed bed reformers, the plate-type reformers have the advantages of more uniform flow, longer residence time of the reactant fluid within the catalyst layer and higher surface-to-volume ratio, which contribute to higher hydrogen yield [93].

Perng et al. [94] investigated the performance of a novel plate-type MSR through CFD, where cylindrical cavities were installed on the bottom of the reformer channels. They found that the novel MSR design showed higher reforming performance and higher net PEMFC output power compared to the traditional plate-type MSRs without the application of cavities. They also found that the higher heated wall temperature and deeper and larger diameter cavities can help to improve the reformer performance with enhanced net PEMFC output power. However, in this case the increase in methanol conversion rate and higher hydrogen content comes with higher CO content in the reformate gas and the cavities can cause higher pressure drop through the channels, which will need additional pumping energy to drive the reactants flow.

Bravo et al. [95] reported a catalyst wall coating applied to a tubular reactor and tested the reformer for 10 days without observing any peeling off the coating. They also found that the catalytic activity of the wall-coated catalyst was better than the packed bed catalyst with the same catalyst. Lee et al. [96] studied the reacting flow transfer phenomenon in the wall-coated and packed bed reformers separately and found that the wall-coated reformer had smaller power requirement for fuel delivery and smaller thermal resistance. The methanol conversion and CO content of these two reformers were the same under the same operation condition. Karim et al. [86] investigated the MSR kinetics and the performance of wall-coated and packed bed reformers with the same commercial catalyst, $CuO/ZnO/Al_2O_3$, through both experiments and modeling. Their results showed that the wall-coated reformer had lower heat and mass transfer limitations, lower pressure drop and higher catalyst activity compared to packed bed reformer. Besides, thicker catalyst wall-coatings contributed to increased volumetric productivity for the same reactor diameter. Chein et al. [97] also reported that the catalyst-layer thickness could greatly affect the fluid flow characteristics, the temperature distribution and the heat and mass transfer. In their study, the wall-coated reformer showed better methanol conversion efficiency than packed bed reformer due to the obtained higher reforming temperature in wall-coated reformer, which however also increases the CO content. Similar results were also found by the Hao et al. [92], who carried out studies on the wall-coated and packed bed reformers separately and found that the wall coated reformer had higher temperature and methanol conversion rate than the packed bed reformer, acquired at the price of increased CO content. Besides, the catalyst layer thickness had indirect effect on the CO concentration in the reformates, optimized wall-coated catalyst thickness ratio of 0.6 was proposed to balance the methanol conversion rate and CO concentration.

Based on the above literature review, the plate-type MSR reformer offer several benefits, such as lower pressure drop, smaller thermal resistance that results in enhanced thermal management of the reformer. These improved heat and mass transfer characteristics also lead to lower transport resistance, fast dynamic operations, higher reforming temperature, and ultimately to higher methanol conversion rate. However, optimization or novel reformer designs should also be carried out with respect to the coating procedure and catalyst replacement for further cost reduction [98].

3.1.3. Membrane MSR

In order to improve the purity of hydrogen in reformate gas and avoid the poisoning effect of the unconverted methanol or the produced CO on the anode catalyst of the fuel cell, membrane reformer design is often used. This design, typically incorporates a thin palladium-based or graphite plate with high hydrogen selectivity and permeability into a catalytic reformer for coupling with PEMFC applications [99–102]. Ribeirinha et al. [103] firstly proposed a novel packed bed membrane reactor integrated with a HT-PEMFC, where a 4 μm thick of Pd–Ag membrane was incorporated between the membrane electrode assembly of HT-PEMFC and the reformer catalyst. The performance of the combined reformer and fuel cell system was investigated through a non-isothermal 3D simulation. The result showed that the performance of the combined unit was comparable to the performance of HT-PEMFC that was supplied with pure hydrogen, where the compact system design allowed efficient heat integration. However, the stability and costs of the Pd–Ag membrane is worth considering. As mentioned above, HT-PEMFC has higher CO tolerance of 30000 ppm, and therefore, the development of membrane reformer is mainly for the integration of MSR reformer with low temperature PEMFC, which has high purity (99.9999%) requirement for the feed hydrogen. Nonetheless, future development should investigate if the utilization of membrane reformer in the

integrated system can increase the lifetime of the MSR-HT-PEMFC system.

3.1.4. Micro/mini structured MSR

Considering the compactness of the MSR system, especially when integrated with the mobile and miniaturized portable fuel cell system applications, micro/mini structured MSR reactors with micro structured features and sub-millimeter dimensions have been investigated recently [104–108]. For micro/mini reformers, the heat transfer efficiency and the reactants flow distribution are critical for the reformer performance. The commonly developed micro reformers are packed bed reformers with small dimensions and microchannel designed reactors. The small-dimension packed bed reformers have the disadvantages of large pressure drop and significant temperature gradient both in axial and radial directions of the bed. To improve the flow distribution and the heat and mass transportation of micro reformers, both experimental and modeling work have been carried out extensively.

Zhang et al. [83] developed a novel multichannel micro packed bed reformer, which has a bifurcation inlet and rectangular outlet manifold. In this new designed micro reformer, the flow distribution uniformity was greatly improved and reached beyond 99.3%, high methanol conversion rate of 94.04% was also achieved with CO content lower than 1.05%. Ataallah Sari et al. [76] established a 3D CFD model to simulate the performance of a microreactor, which consist of 13 structured parallel channels. Their results showed that these narrow channels contribute to high hydrogen production rate as well as low CO content, and the reformer with cylindrical microchannels showed better performance than that with rectangular microchannels. Zhang et al. [109] investigated a cross-u type micro MSR reformer, which consists of a reformer and a combustor, both experimentally and numerically. The results showed that compared to the conventional tubular and parallel-U type micro reformer, this novel structure design showed better performance on thermal efficiency and methanol conversion rate with acceptable CO content in the reformate as feed gas for HT-PEMFCs. Kang et al. [110] analyzed the performance of both types of packed bed microchannel reactors with different microchannel designs, such as the cross-section shape and flow distributions, as well as plate-type microchannel reformers. They found that the structure and distribution of the microchannels of the reformer play an important role in the performance of the micro MSR. Besides, the reformer size, the assembly type, the surface shape and the catalyst loading are also important factors that affect the performance of the micro structured reformers.

Compared with the conventional chemical reactors, the micro/mini structured reactors have the advantages of higher surface-to-volume ratio, better heat and mass transfer properties, rapid response time, ease of control of the operation parameters such as temperature, flow rate, and residence time, making it suitable to integrate with a fuel cell [104,111]. However, the cost and time required to design and construct these small MSR reactors are high.

3.1.5. Other design optimizations

Evaporator integration is necessary in an MSR-HT-PEMFC system as the methanol and water mixture needs to be heated to steam phase to perform the methanol steam reforming reaction. Therefore, the evaporator configuration could be an important factor to the MSR-HT-PEMFC system efficiency. Yu et al. [112] investigated two different evaporator configurations in the MSR-HT-PEMFC system, with one system with external evaporator as reference and the other one with internal evaporator. The two MSR-HT-PEMFC systems were operated by changing the heat duty and steam to carbon ratio. Results showed that the waste energy was reduced for the reformer and the system thermal efficiency was improved with the internal evaporator configuration.

3.2. External MSR-HT-PEMFC integration

The working temperature of HT-PEMFC is typically 160 °C, while the operating temperature of MSR process is usually above 250 °C. The temperature mismatch of fuel cell and reformer lead to the development of the external integration of MSR-HT-PEMFC system, where the reformer and fuel cell work as separate subsystems at different working temperatures in the system.

Herdem et al. [113] investigated the performance of a methanol reformate gas-fueled HT-PEMFC system through modeling. The schematic of the MSR-HT-PEMFC system, as shown in Fig. 4, mainly consist of the MSR reformer, a combustor, an evaporator and a HT-PEMFC stack. The operating temperatures of the stack and reformer can significantly affect the system efficiency due to the change in the CO molar ratio in the reformate gas, where a maximum system efficiency of

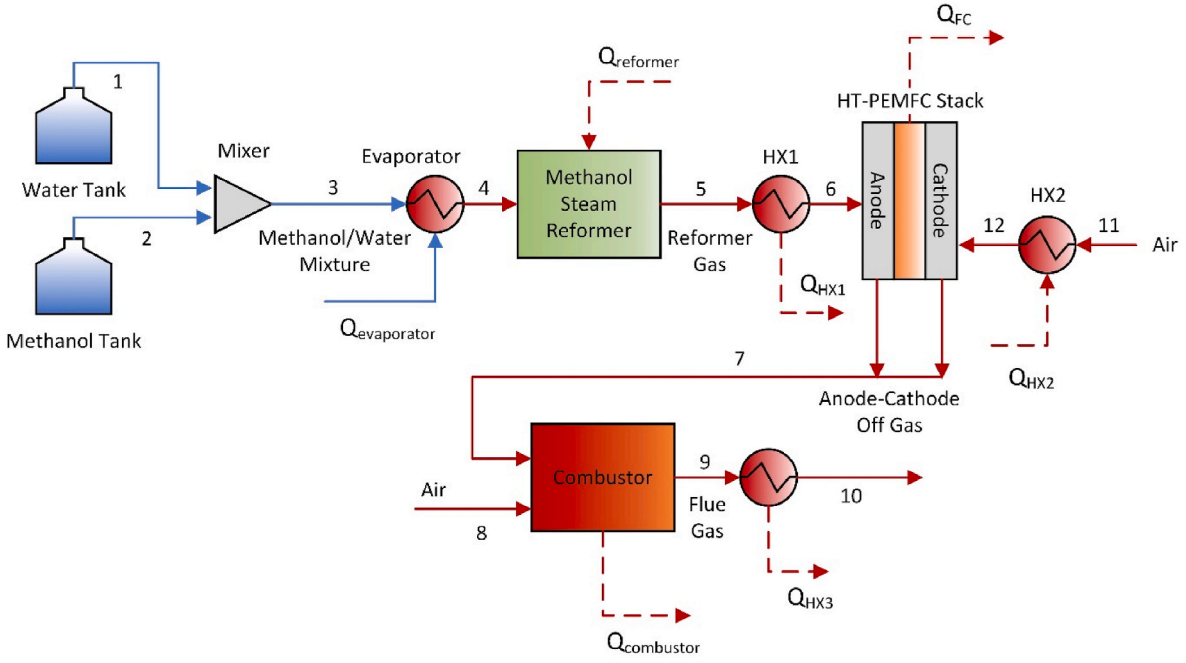

Fig. 4. Schematic of the methanol reformer system (reproduced from Ref. [113]).

Table 7
Literature review of external integrated MSR-HT-PEMFC system.

Publication year	Reformer type/catalyst	T of MSR (°C)	T of HT-PEMFC (°C)	Power output (W)	Methanol conversion rate	System efficiency	Methods	Ref.
2010	Micro fuel processor MSR reformer/Base and noble metal catalysts	250–285	180	30	94%	–	Experiment	[114]
2014	Micro-combined MSR reformer/Interior	300	150–180	1000	–	18.46–26.41% for different H_2 utilization 23.74–33.60% for different fuel cells operation temperature	Modeling	[115]
2015	Packed bed MSR reformer	180	150	5000	–	28–30%	Modeling and experiment	[47]
2015	Senergy H3-350/CuZn	240–300	160–180	450	–	27%–35%	Modeling	[113]
2017	Micro structured MSR reformer/CuZnGaOx	200	185	8.5	98.5%	21.7%–35.5%	Modeling and experiment	[116]
2017	Packed bed MSR reactor/CuO/ZnO/Al_2O_3 (BASF RP-60)	180	175–185	427	88–100%	–	Experiment	[117]
2021	Microreactor MSR reformer/Cu/ZnO/Al_2O_3	208–225	160	109.3	94%		Modeling	[118]
2020	$Cu_2O/Ca_2Fe_2O_5$	160–200	120–180	–	–	21.6%–26.7% for start-up, 47.7% for working stages	Modeling	[119]

35% was obtained at the stack operating temperature of 180 °C and the reformer operating temperature of 240 °C. Sahlin et al. [47] investigated 5 kW HT-PEMFC system with an integrated external methanol reformer, which consisted of similar components of burner, reformer, evaporator and fuel cell. Through dynamic modeling and experimental work on the reformer, the efficiency and the start-up time of the system were estimated to be around of 28% – 30% and 45 min, respectively. Literature review about externally integrated MSR-HT-PEMFC system, including reformer type, main operating conditions, methanol conversion rate, system efficiency and research methods are summarized in Table 7. It can be seen that the research interests on external system integration have been increasing since 2010. Some improvement on system efficiency has been achieved and should be further enhanced.

To optimize the thermal efficiency of the MSR-HT-PEMFC system Schuller et al. [68] designed a novel MSR reformer, which was integrated with a 12-cell HT-PEMFC stack. The reformer used in this system was a heat exchanger MSR reformer (HER) packed with the commercial CuO/ZnO/Al_2O_3 catalyst to obtain the MSR reaction. The heat produced by the stack was routed to the HER through the coolant loop to power the methanol reforming process as shown in the process diagram in Fig. 5. Both the stack and reformer in this system were operated at the same operating temperature of 180 °C with a CO content below 0.5% vol in the reformate gas. This demonstrated that the heat released from the stack is sufficient to obtain a methanol conversion in the HER through a liquid coolant circuit, resulting in a total heat utilization of 86.4% for the HT-PEMFC stack.

External integration of MSR-HT-PEMFC system has no special component design and catalyst requirement for both fuel cell and reformer. The reformer can operate at high working temperature to keep high methanol conversion rate and reduce unreacted methanol content in the reformates. However, the external integration cannot make use of the heat released from the electrochemical reactions occurring in the system for the MSR reaction, leading to quite low system thermal efficiency and long start-up time as shown in Table 7. Besides, independent reformer and fuel cell operation need other auxiliary components such as evaporator, heat exchanger, condenser, etc. to ensure the proper temperature and fuel control in the system, which lead to uncompact system design.

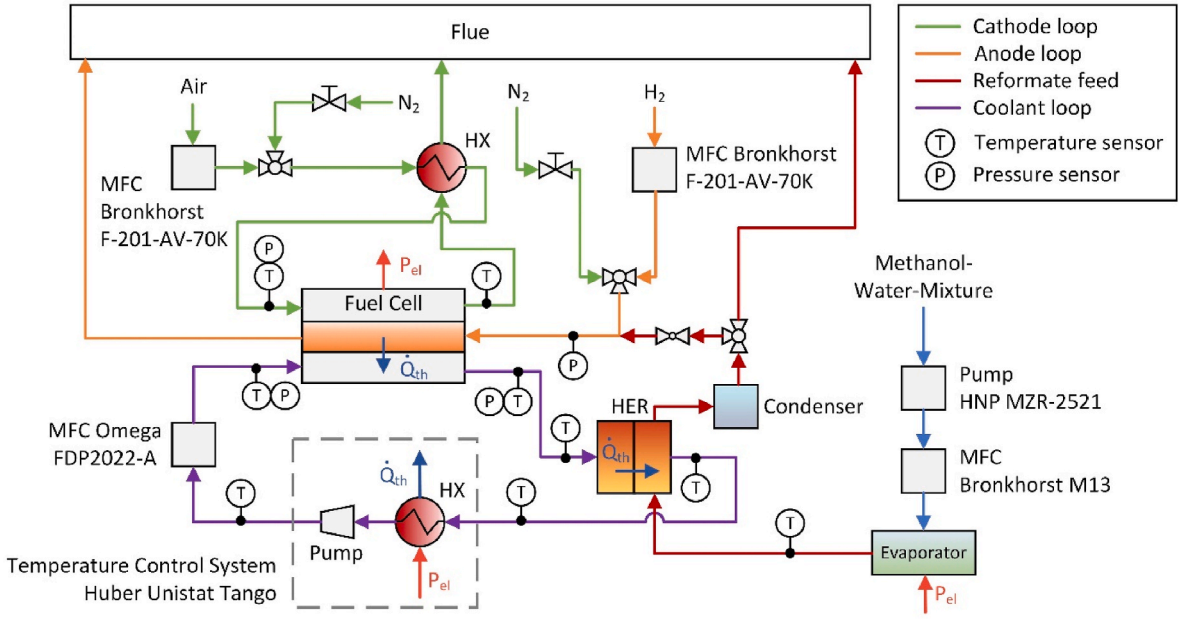

Fig. 5. Flow chart of the integrated MSR-HT-PEMFC system (reproduced from Ref. [68]).

Table 8
Literature review of internal integrated MSR-HT-PEMFC systems.

MEA	Reformer	Temperature (°C)	Power (W cm^{-2})	MeOH conversion	Main results	Ref.
ADVENT TPS® MEA	CuMnOx/Cu foam	200	0.12	>90%	Unreacted methanol poisons the anode electrode.	[27]
Homemade m-PBI membrane	CuO/ZnO/Al_2O_3 catalyst	180–200	0.45–0.55	>90%	Less than 10% decline after 100 h operation. Low stability of the IRMFC single cell at high current density.	[89]
TPS®phosphoric acid-doped copolymer	Cu–Mn spinel oxide supported on metallic copper foam	200	0.1315	>75%	No performance degradation for more than 72 h.	[121]
TPS® membrane	CuZnAlOx methanol reforming catalyst carbon paper	200–210	0.114	>95%	Gradual stack performance degradation was observed after each start-up step.	[122]
Advent®MEA	Ultrathin reformer based on catalyst (HiFuel R120) /Indirect contact with fuel cell	160–220	0.1284	>90%	Efficiently operated for more than 72 h at 210 °C.	[123]
ADVENT TPS-H_3PO_4-doped copolymer	$CuMnO_x$ catalyst supported on metallic copper foam	200	–	–	30% decline in MeOH conversion after 350 h operation.	[19]
Celtec®P2200 N MEA	CuO/ZnO/Al_2O_3 (BASF RP60)	180/190/200	–	96%	The device demonstrated quite good stability at high operating temperature and showed a degradation rate of 100 μV h^{-1} at 180 °C after 700 h operation.	[53]
ADVENT cross-linked TPS®MEA	Al-doped $CuMnO_x$ catalyst supported on metallic copper foam /Indirect contact with anode	200–210	–	>95%	Stable operation at a conversion level higher than 95%.	[124]
Serenergy A/S	Heat exchanger reformer filled with CuO/ZnO/Al_2O_3 (BASF RP-60)	180	2.59	100	The system was operated up to 0.4 A cm^{-2} generating an electrical power output of 427Wel. A total stack waste heat utilization of 86.4% was achieved.	[117]
Advent TPS®MEA	BASF (RP-60)	180	–	>90%	Methanol slip led to MEA degradation	[70]
Celtec P2200 N MEA	CuO/ZnO/Al_2O_3) from BASF (RP-60)	160–200	–	>95%	A novel integrated MSR-C/HT-PEM stack with ten cells was proposed and simulated, showing a performance above the reported in the literature for similar devices	[125]
Celtec P2200 N MEA (BASF)	CuO/ZnO/Al_2O_3 BASF (RP-60)	160–200	–	89%	Pd–Ag membrane was included to avoid methanol poisoning, high performance and efficient heat integration was achieved.	[52]

3.3. Internal MSR-HT-PEMFC integration

To configure a compact MSR-HT-PEMFC system design by avoiding too many components for each separate subsystem and to improve the thermal efficiency of the system, internal MSR-HT-PEMFC system integration was proposed and studied by many researchers as summarized in Table 8. Avgouropoulos et al. [120] developed an internal MSR-HT-PEMFC setup with a two-layer bipolar plate providing methanol reforming reaction compartment on one side and hydrogen oxidation reaction on the other side. The electrochemical test results showed that the fuel cell performance decreased compared to pure H_2 as fuel due to anode catalyst and membrane poisoning caused by the unreacted methanol slip and crossover. Moreover, the methanol conversion along the flow direction was not uniform, which was low at the inlet and high at the outlet. A Kapton film was employed in the reformer compartment to optimize the methanol conversion and improve the cell performance.

Similar internal MSR-HT-PEMFC system design was also studied by Ribeirinha et al. [75]. They developed a 3D model to simulate the integrated reformed methanol HT-PEMFC and proposed a novel integrated system consisting of 10 cell-stack as shown in Fig. 6, which has a novel bipolar plate design. This two-sided bipolar plate acted both as flow plate for fuel cell on one side and flow field for reformer on the other side. The anode off-gas was fed to the burner as fuel and the device temperature was controlled by changing the cathode stoichiometry. No external heating was added to the system, but the operating temperature of the system increased with the current density, which makes the temperature control of the system inflexible. It is worth noting that the operating temperature of the system can only be within the limited temperature range to balance methanol conversion rate and fuel cell performance.

As can be seen from Fig. 6, the general design of this internal MSR-HT-PEMFC system integration is the incorporation of methanol reformer into the anode of the HT-PEMFCs through a bifunctional plate, which separates the methanol steam reforming reaction in the reformer and the hydrogen oxidation reaction in the anode of the fuel cell. This design can better recover the waste heat of HT-PEMFCs for methanol reforming reaction, which improves the energy efficiency of the system. Therefore, the internal integrated design avoids other auxiliary system components, such as heat exchangers, simplifying the whole system setup and minimizing the weight and volume of the integrated system.

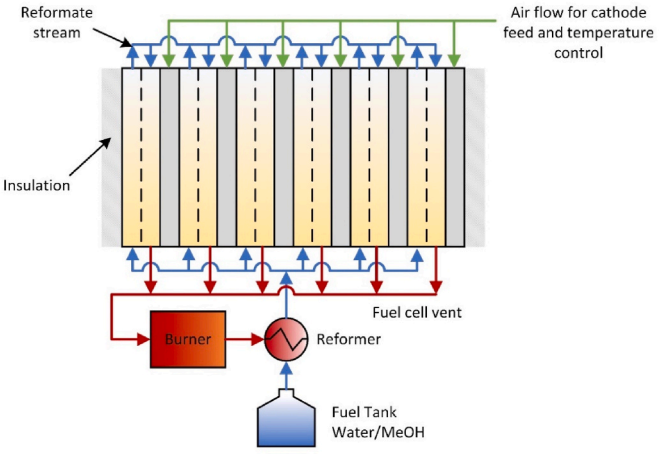

Fig. 6. Novel designed MSR-HT-PEMFC stack (reproduced from Ref. [75]).

However, there are also some problems that come with this internal configuration: (1) the working temperature of the system is limited because temperatures higher than 200 °C can improve the methanol conversion rate but lead to severe degradation of HT-PEMFCs, while

temperatures below 200 °C will lead to low methanol conversion rate and large amount of catalyst are necessary to obtain acceptable methanol conversion rate at operating temperature lower than 200 °C; (2) methanol slip and crossover phenomena cannot be avoided due to the presence of the unreacted methanol, which can also poison the anode catalyst and the membrane, leading to poor catalyst activity and membrane conductivity in the fuel cell; (3) the catalysts in the reformer can be released to the membrane of the fuel cell, which will lead to the phosphoric acid leaching from the membrane.

To alleviate the above-mentioned problems, researchers have made efforts on advanced catalysts investigation. Avgouropoulos et al. [126] prepared an Al-doped CuMnOx catalyst with high activity, which allowed methanol reforming reaction to occur at about 200 °C – 210 °C with high methanol conversion rate. Ribeirinha et al. [45] introduced an expansion vessel in the integrated system to reduce the oscillation of the flow rate, which they reported can significantly increase the methanol conversion rate. A separation layer with different materials is usually employed between the reformer catalyst and the anode electrode of the fuel cell to protect both catalysts of reformer and fuel cell from the poisoning by unreacted methanol and phosphoric acid leaching [124, 126–128].

3.4. Two-stage temperature MSR-HT-PEMFC integration

To optimize the system efficiency and improve the thermal management of the integrated system, a two-stage temperature integration of the steam reformer and PBI membrane fuel cell system was proposed by Weng et al. [129]. Their system included an internal one-stage temperature steam reformer that was integrated with the fuel cell and an extra reformer that was externally integrated with the one-stage temperature system integration to make the two-stage temperature MSR-HT-PEMFC integration system, as shown in Fig. 7. The internal reformer operated at 190 °C to make use of the heat produced by fuel cell and the external reformer utilized the fuel cell tail gas to heat the reformer to 240 °C. The performance tests showed that the two-stage system integration was more stable and more efficient than the one-stage integrated system, where the methanol conversion rate and the hydrogen concentration were both improved for the two-stage system integration compared to the one-stage integrated configuration.

3.5. Trigeneration system

To improve the energy utilization efficiency and energy supply renewability, an integrated trigeneration system consisting of a solar heat collector subsystem, a MSR subsystem, a phosphoric acid fuel cell (PAFC) power generation subsystem and heat recovery utilization subsystem as shown in Fig. 8 was proposed by Wang et al. [130]. The heat collected from the solar collection system was sent to the reformer to carry out the MSR reaction, the heat transfer oil from the reformer delivered heat to the superheater to produce steam in the steam generator. While the waste heat released from fuel cell and the steam heat from the steam generator were used to drive the absorption heater/chiller for heating or cooling demands depending on the weather. Besides the heat recovery in the system, cyclic utilization of the water produced in the MSR reaction was also obtained in this trigeneration system. The thermodynamic simulation showed a system energy efficiency of 73.7% and 51.7% during summer and winter, respectively. However, the solar heat collection efficiency is still an issue, of which the exergy destruction and loss accounted for 41.9% and 34.1% of the total loss in the system in summer and winter, respectively.

Sarabchi et al. [10] proposed two novel cogeneration systems that consist of HT-PEMFC, methanol steam reformer and a Kalina cycle. The difference between these two-cogeneration systems is where the heat used for methanol steam reforming comes from, where one was from a catalytic combustor integrated with the MSR reformer, the other was from a coupled parabolic trough solar collector with a heat storage tank. The waste heat released from the HT-PEMFC was used to drive the Kalina cycle to produce domestic hot water. The integration of solar energy with the MSR-HT-PEMFC system contributed to better environmental and economic performance and reduced the fuel consumption by 34%.

4. Control and diagnosis

The MSR-HT-PEMFC system is a coupled multi-physics system that consists of electrochemical reactions, mass and heat transfer, fluid flow, etc. The performance of each process can affect the performance and efficiency of the whole system. Therefore, proper operating parameters control, such as the fuel flow rate, operating temperature, load changes, etc., and system diagnosis are necessary for the MSR-HT-PEMFC system. The streams of mass, heat and electricity (or electrical signal) and their connections with the main components for a typical MSR-HT-PEMFC system with control and diagnosis subsystems are shown in Fig. 9.

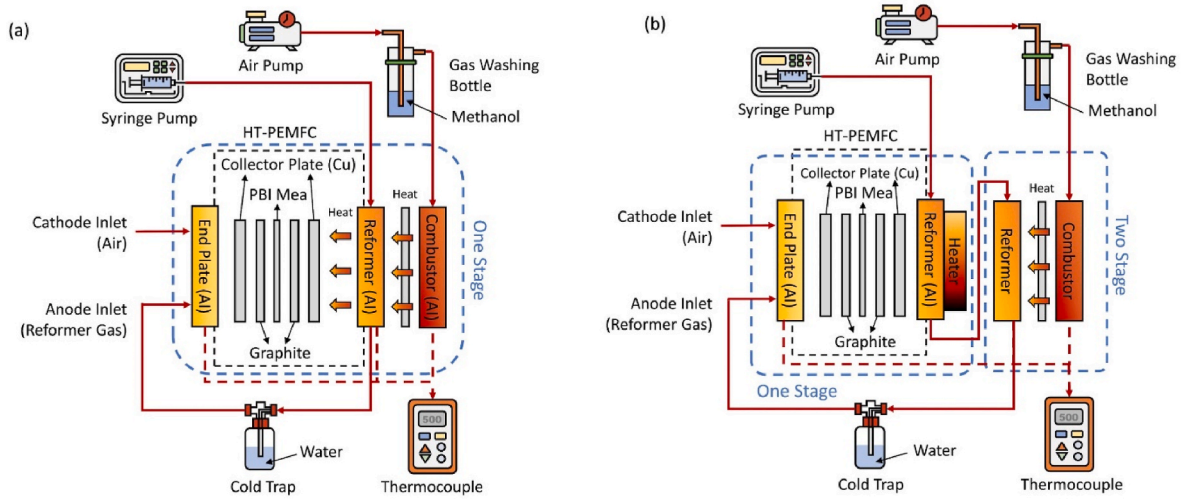

Fig. 7. (a) The one-stage MSR-HT-PEMFC system and (b) two-stage MSR-HT-PEMFC system (reproduced from Ref. [129]).

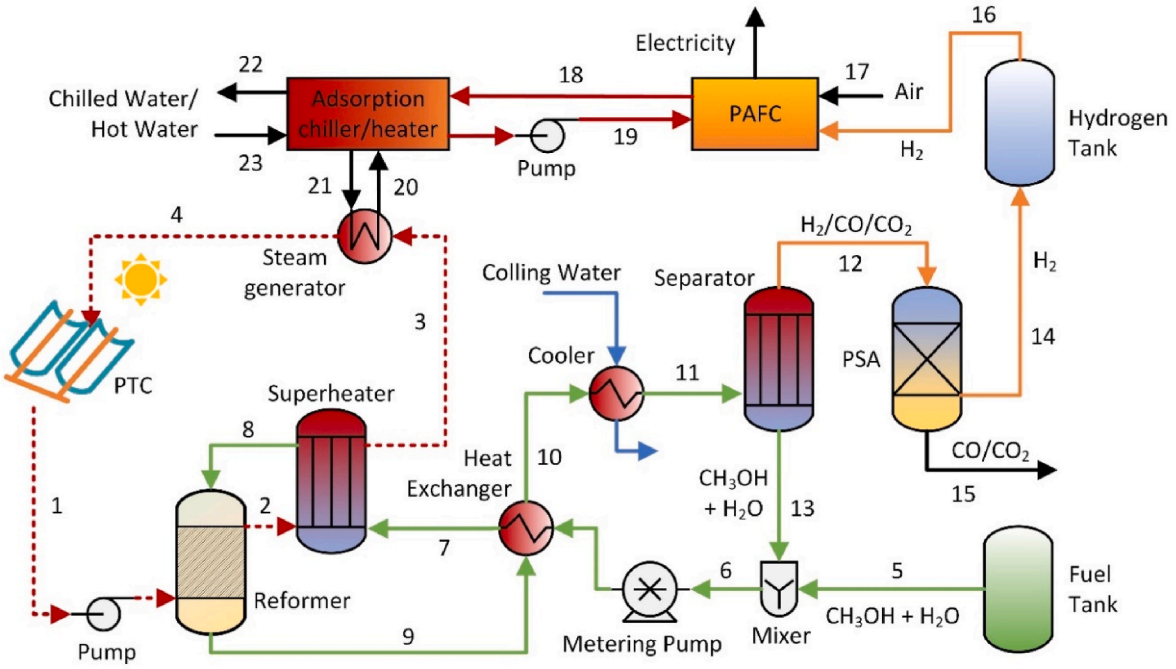

Fig. 8. Schematic of the trigeneration system (reproduced from Ref. [130]).

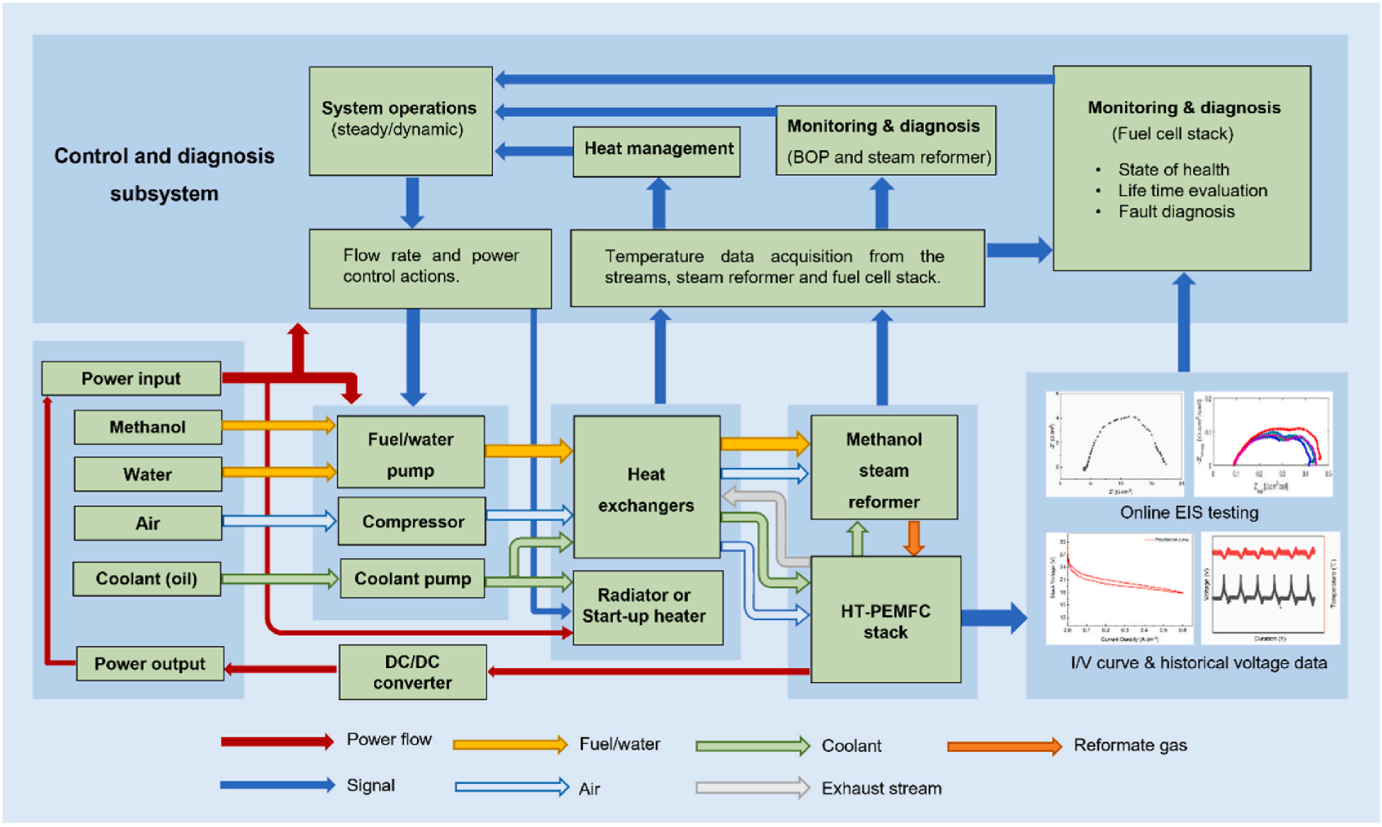

Fig. 9. Scheme of a typical MSR-HT-PEMFC system with control and diagnosis subsystems.

4.1. *Dynamics of the MSR-HT-PEMFC system*

Several studies have evaluated the fuel cell performance at steady state operation. However, during real-world applications, fuel cell systems may also experience dynamic conditions, such as startup-shutdown, load change, idle to full power, and emergency stops. There is a lag of the heat transfer from the burner to the reformer, which affects the methanol conversion in the reformer [131]. Sahlin et al. [47] developed a dynamic model to study the efficiency, the stability and the response time of the system for load change from 0 to 5 kW together with

experimental validation. The results showed that it took the system about 45 min to startup and the system efficiency was around 28% – 30%. Besides, a 10 s delay was found from the methanol pump to the fuel cell during the load changes.

If the hydrogen (hydrogen rich reformate gas) supply rate to the fuel cell is lower than what the load change requires due to slower dynamics of the reformer and gas flows to the fuel cell compared to load change, the fuel cell will suffer from the fuel starvation, thereby degrading the fuel cell by cell reversal mechanism [132,133]. Besides, if the system experiences sudden stop or lower load, the hydrogen (hydrogen rich reformate gas) supplied to fuel cell goes directly to the burner, and thus leading to high burner temperature and burner catalyst deactivation that may cause stability issues in the system. Therefore, it is essential to control properly the operating parameters such as the temperature, pressure, flow rate of the methanol-water mixture stream as well as fuel cell load, during operation. The investigation on the whole system dynamics is necessary and valuable for control design and optimization of the operating parameters.

4.2. Temperature and load control

The fact that the operating temperatures of the fuel cell and the reformer in the MSR-HT-PEMFC system are usually different can present some challenges for the thermal integration of the system. There is usually a cooling system to keep the desired operating temperature, typically with liquid (oil) or air as coolant. The liquid cooling system requires cooling channels and additional components in the system for circulation, no special compressor and blower are required, and the temperature distribution is more uniform for liquid cooling system [134,135]. For air cooled system, the system temperature is controlled by adjusting the air supply to the system, and while cooling channels for coolant are not necessary, flow field and manifolds optimization are needed to keep low pressure drops in the system [135]. The cell temperature uniformity is another challenge for air-cooled systems [136].

As can be expected the behavior of the reformer will be greatly affected by different operating conditions. Higher operating temperature can lead to high methanol conversion but increased CO content. Vice versa, lower reforming temperature will lead to lower methanol conversion, resulting in lower CO content and higher content of unconverted methanol in the reformates. Since both CO and methanol in the reformate can poison the anode of the fuel cell [44,45], a proper control of the reformer operating temperature is of paramount importance. Stamps et al. [137] used two low-level proportional integral (PI) control loops for the temperature control of the reformer and PEMFC stack. In practice, the reformer temperature was controlled by adjusting the wall temperature through a valve controlling the fuel flow, while the fuel cell temperature is controlled by adjusting the flow rate of the coolant. Andreasen et al. [64] proposed a cascade control strategy in a study of 350 W HT-PEMFC mobile battery charger of Serenergy H3-350, where an inner and an outer negative feedback control loops were used to control the temperature of the burner and reformer, respectively as shown in Fig. 10. During the reforming process, the reformer temperature can be well controlled by changing the value of $T_{Reformer,\ Setpoint}$ or the fuel flow of methanol and water mixture, which quickly changed the burner setpoint temperature of $T_{Burner,\ Setpoint}$, and then the burner temperature was effectively controlled by adjusting the value of the volumetric flow rate of air, $_{Burner,air}$.

Justesen et al. [138] developed an output current controller based on a dynamic model. In their study, a dynamic model was built to simulate the differences between the setpoint current and the output current of the reformed methanol fuel cell system, caused by the energy consumption of the balance of plant. A PI controller consisting of feedforward and anti-windup was then designed to control the output current of the system. Physical system test and verification showed that the controller functioned as intended for the reformed methanol fuel cell system.

4.3. MSR-HT-PEMFC system diagnosis and fault tolerant control

Diagnosis in fuel cells is very important in order to minimize degradation and enhance their reliability and availability. Even though, in literature diagnosis and characterization are used interchangeably, here diagnosis is fault detection and identification followed by fault mitigation. There have been numerous studies on diagnostic techniques

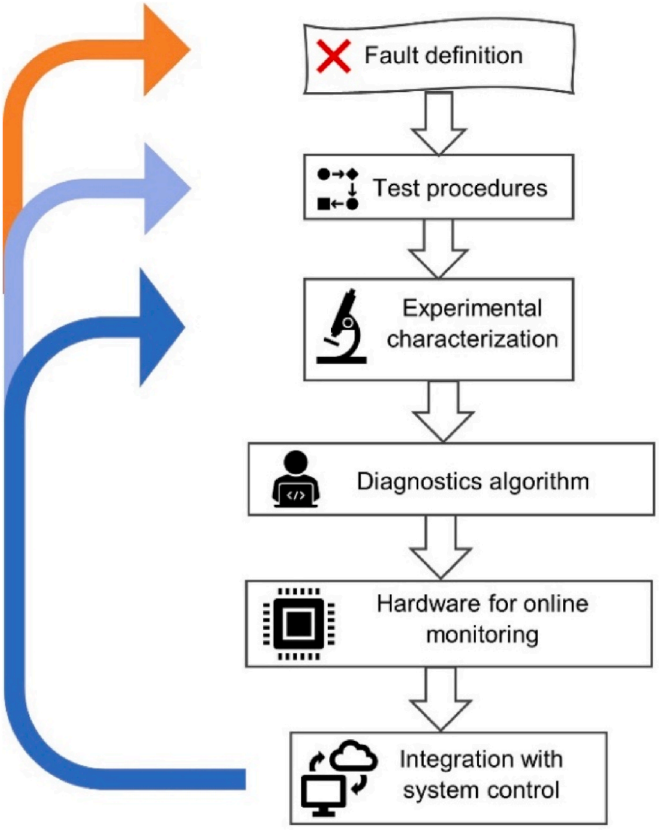

Fig. 11. Steps for the development of diagnostic tool [144].

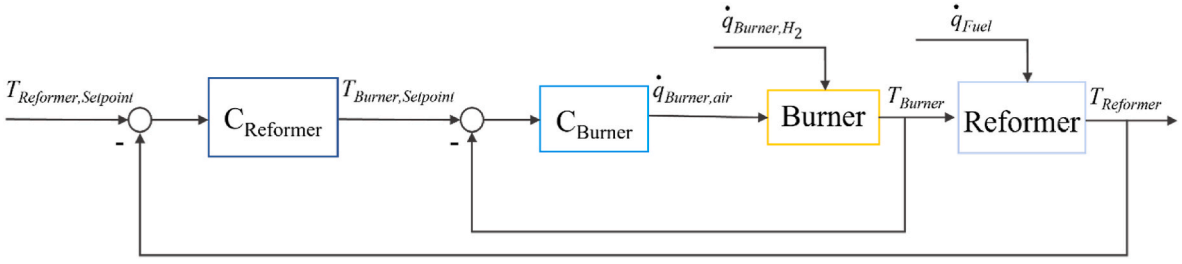

Fig. 10. Flow chart of the control strategy (reproduced from Ref. [64]).

for LT-PEMFC [139–142], including for online diagnosis. However, the literature on HT-PEMFC diagnosis is scarce, perhaps due to lower maturity of the technology compared to LT-PEMFC, even though they suffer from higher degradation rates due to harsher operating conditions of higher temperature and reformate impurities. Nonetheless, fault detection and isolation along with diagnosis and fault tolerant control strategies are crucial to timely mitigate fuel cell faults and improve their reliability and availability, and to enhance their durability [143]. For the above-mentioned reasons, this is especially important for HT-PEMFC.

The typical steps for the development of a diagnostics tool are illustrated in Fig. 11. When preparing a diagnostic tool, techniques for monitoring these faults are determined and test procedures are prepared to investigate the response of the fuel cell system to different intensities of the faults. From these, fault patterns and features are identified and a fault matrix is prepared. The diagnosis approach for fault detection and isolation (FDI) can be residual-based, data-based or knowledge-based [143]. Finally, for the diagnostic tool to work properly, targeted faults need to be defined and their characterization method must be identified. Furthermore, for the tool to be useful, corrective measures need to be implemented into the control system to mitigate the fault or if lifetime estimation is done based on degradation mechanisms a predictive maintenance can be planned.

Diagnosis should preferably take place during the system operation without compromising the availability of the system and without disturbing the system's steady state operation. Therefore, the measurement techniques chosen to quantify the parameters needed for fault detection should be easy to implement online and should not interfere with the system's integrity. For this reason, parameters such as temperature, pressure, voltage and impedance are best suited for diagnosis. Among electrochemical characterization techniques, electrochemical impedance spectroscopy (EIS), which only superimposes small alternating current (AC) amplitude to the direct current (DC) load without causing any degradation, is the most suitable for the detection and identification of several faults. Because it not only causes the least disturbance to the normal operation of the fuel cell system, but also allows to distinguish some of the contribution of the different process in the fuel cell according to frequency range and phase angles. Moreover, it can be implemented for online monitoring on the DC-DC converter of the power supply as the EU funded project Health-Code demonstrated [145].

The main faults in HT-PEMFC are caused by impurities poisoning of the anode catalyst and the membrane when reformer is used to provide hydrogen rich gas to the fuel cell, and by reactants starvation. These can be caused by a malfunction in the reformer, such us catalyst deactivation and improper operating conditions of temperature and flow rates. Jeppesen et al. [138] used artificial neural network (ANN) based algorithm to train, label and classify faults based on EIS data on a small stack. They identified 5 different faults, namely low and high cathode stoichiometric ratio, high CO and high methanol concentration in the anode feed and low anode stoichiometric ratio (fuel starvation). Their FDI algorithm was based on artificial neural network classifier with three extracted fault features, two of which were degradation independent as they were based on angles in the Nyquist plots. The steps of their FDI algorithm are shown in Fig. 12. The same authors developed a current pulse injection (CPI) method as a quick alternative for EIS for online implementation [146].

Table 9 summarizes the cause of each of the main faults in reformed methanol-fed HT-PEMFC, their effects on the fuel cell system along with their identifying features and mitigation strategies. From the nature of the faults and their identification features it can be seen that even if the faults are observed in the fuel cell, most of the causes of the faults originate in the reformer. Consequently, most of the mitigation actions are done on the reformer, which calls for a close integration of the fuel cell diagnosis system and the reformer control system in a tightly integrated overall MSR-HT-PEMFC system.

5. Application

By combining both the methanol economy and hydrogen economy during this era of green transition, the MSR-HT-PEMFC system shows great potential for several applications, including transportation, stationary, and portable applications. Since PBI-based membrane was firstly suggested as an electrolyte for HT-PEMFC [148], it took around two decades for the technology to develop from lab scale to

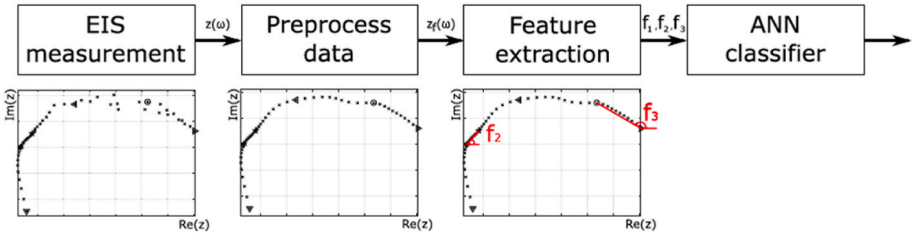

Fig. 12. Steps of FDI algorithm for an HT-PEMFC stack [147].

Table 9
The main faults in HT-PEMFC systems; their causes and effects; identifying features and mitigations strategies.

Faults	Cause	Effect	Feature to monitor	Mitigation strategy
CO poisoning	- Lower fuel flowrate - Higher reformer temperature	- Loss of active area	- Increase in reformer temperature - Increase in High frequency resistance (EIS)	- Increase fuel flowrate - Decrease reformer operating temperature - Lower fuel cell load - Air bleeding
CH_3OH Poisoning	- Higher fuel flowrate - Lower reformer temperature	- Membrane degradation	- Decrease in reformer temperature - Increase in intermediate and ohmic resistance (EIS)	- Adjust reformer temperature - Adjust fuel flowrate
Anode starvation	- Reformer malfunction - Flow channel blockage	- Cell reversal - Loss of active area/Catalyst corrosion - Catalyst support and gas diffusion layer (GDL) corrosion	- Reformer performance and temperature profile - Increase in low frequency resistance (EIS)	- Fix reformer operating conditions - Increase fuel flow to the reformer to increase anode stoichiometric ratio
Cathode starvation	- Compressor malfunction - Flow channel blockage	- Hydrogen crossover - Catalyst and membrane degradation by radicals' attack	- Lower stack voltage - Increase in low frequency resistance (EIS)	- Increase air flowrate - Maintenance

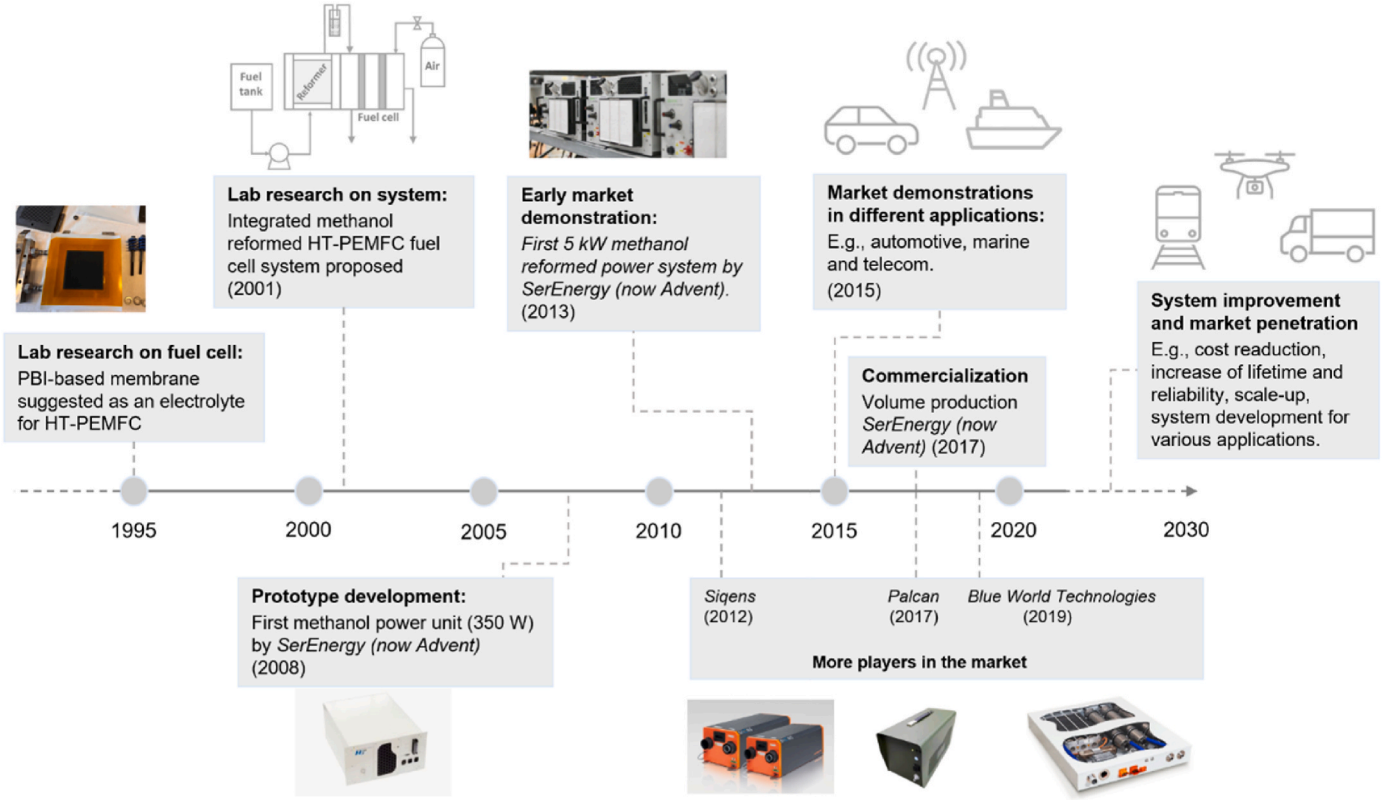

Fig. 13. Development of MSR-HT-PEMFC system: from lab to market [149–153].

commercialization (as shown in Fig. 13). Growing commercial activities have been reported in recent years with systems of up to hundreds of kW. The potential applications for this system are still expanding in different sectors, such as transportation, including heavy duty; stationary, including backup for telecom and other critical applications, auxiliary power unit (APU), and residential combined heat and power (CHP) supply.

5.1. Transportation applications

The transportation sector contributes to 37% of the CO_2 emissions from end-use sectors worldwide [154]. Therefore, there is great demand to develop emission reduction technologies for automotive applications such as fuel cell systems. The share of fuel cell electric vehicles (FCEVs) is currently very small at $< 0.01\%$ [155] of the global stock of total vehicles. However, significant market expansion of FCEVs is expected, with around 6 million FCEVs on the road by 2030 [155]. LT-PEMFC is currently the main technology employed in FCEV market, including passenger vehicles like the Toyota Mirai. HT-PEMFC systems are still in a preliminary stage of commercialization. The higher operating temperature (e.g., 160 °C) of HT-PEMFC results in a longer start-up time, which poses challenge for its use in automobiles as the main power source. However, HT-PEMFC integrated with methanol steam reforming (MSR-HT-PEMFC) showed growing commercial potentials in automotive applications as range-extenders for hybrid power systems (e.g., battery/fuel cell system, as shown in Fig. 14) [153] and auxiliary power units (APU) [153]. The former application was reported to provide up to 1000 km of range for passenger vehicles [153] by the Danish-based company Blue World Technologies, while the ranges for typical all-electric vehicles based on lithium-ion batteries in the market was reported to be less than 750 km. Furthermore, the range extender solution ensures fast refueling due to the use of liquid methanol as fuel. Compared to other range extender technologies, the MSR-HT-PEMFC system provides lower noise and vibration, low harmful emissions, and low CO_2 emissions if green methanol is used [156]. The possible on-road APU applications for MSR-HT-PEMFC were given by Liu et al. [157] with several scenarios mentioned, e.g., idling of heavy-duty and refrigeration trucks. Regarding the commercialization aspect, there are several companies developing MSR-HT-PEMFC systems for transportation applications, including for passenger car and marine vessels by Blue World Technologies [153], for heavy-duty truck by Advent [150] and for truck by Palcan [151], as shown in Table 10.

Besides on-road applications, there is also a great potential in the marine subsector for MSR-HT-PEMFC systems. The recent research project BlueDolphin [158,159] is developing a scalable MSR-HT-PEMFC range-extender platform for small vessels, e.g., workboats. In the Marine fuel cell APU project [160], a 200 kW MSR-HT-PEMFC system with a scalability of up to 5 MW has been proposed for APU on marine vessels. Early demonstration projects with fuel cell power ranging from 5 kW to 35 kW were also summarized by Araya et al. [161].

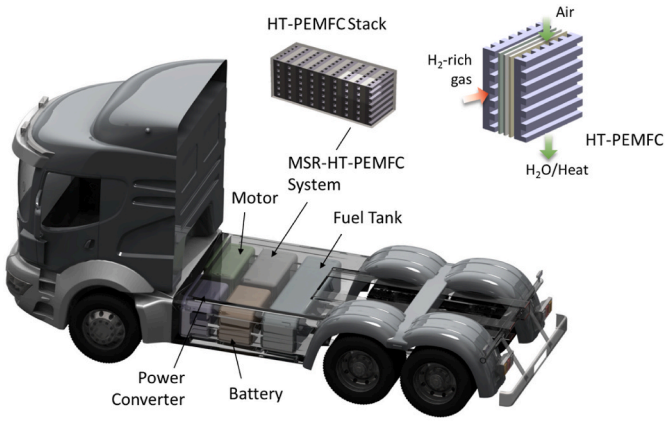

Fig. 14. Schematic of MSR-HT-PEMFC/Battery hybrid system for vehicles.

Table 10
Commercial applications of MSR-HT-PEMFC systems in the market [150–153].

Company	Country	Power	Applications
Blue World Technologies	Denmark	7–25 kW 200 kW–5 MW	• Range-extenders for cars and marine vessels • APU for marine vessels
Advent	U.S./Denmark	50 W 5–15 kW 120–240 kW	• Portable battery charger for military use • Stationary power generation • Range-extender for heavy-duty truck
Palcan	China	300 W 5 kW 20 kW	• Battery charger • Stationary power generation • Range-extender for truck
Siqens	Germany	800 W–4.8 kW	• Stationary and portable power generation

5.2. Stationary and portable applications

In general, fuel cells have been reported to be potential candidates for various stationary applications, such as providing highly reliable power for the telecommunication industry as backup sources, or auxiliary power or primary power for remote areas without grid connection or with unstable grid connection [162]. The MSR-HT-PEMFC system as a fuel cell technology also shows great potential in the above fields, and the commercial products in the market have been reported to be based on 5 kW unit and can be further scaled up [163,164]. Similarly, to the transportation applications, MSR-HT-PEMFC systems for stationary application also shows advantages, including lower noise and vibration, and low harmful emissions compared with systems based on diesel generator. Furthermore, the system can also tolerate extreme weather conditions, e.g., a solution named H3 Outdoor Cabinet has been developed in the research project (Supplemental Power Generation [165]), which can be operated at a temperature range of −20 °C to 50 °C [166]. The recent MFC MultiGen project plans to develop a 5 kW system for APU applications focusing on stack and system components, lifetime, water recycling and dynamic reliability [167]. The European project EMPOWER is aimed at developing, manufacturing and validating a 5 kW combined heat and power system considering fast dynamic response and thermal integration aspects [168]. Early research projects were also found in Ref. [161].

With respect to the portable sector, there are various possible applications for the MSR-HT-PEMFC system, e.g., charger for electronics, outdoor APUs and military uses [162]. Several commercial products can be found in the market with various power levels, e.g., battery chargers with power of 50 W (Advent), 300 W (Palcan) and 800–4800 W (Siqens) (also shown in Table 10). A smaller 30 W power generator at research level was also reported for powering a laptop [14].

6. Future prospects

This section elaborates the technical challenges of the MSR-HT-PEMFC and HT-PEMFC systems in future energy scenarios. Although both transportation and stationary applications of the MSR-HT-PEMFC system have been reported, there are still challenges to be overcome for developing competitive and successful products based on the MSR-HT-PEMFC system, including system lifetime, durability, reliability, efficiency, and cost reduction, among which the lifetime and durability of the system are considered of main concern in future development. The system should demonstrate lifetime of 5000 h (temperature cycle resistance >30000 h) for automotive applications and 40000 h (temperature cycle resistance >4000 h) for stationary applications [169]. The lifetime of MSR-HT-PEMFC system is mainly determined by the HT-PEMFC stacks (e.g., lifetime of 10000 h – 20000 h reported in Ref. [170]), while other components could be used for several years (e.g., 5 – 20 years [170]). Long-term stability (in lab) of more than 20000 h was reported for the membrane electrode assemblies (MEAs) for HT-PEMFC in Ref. [171] and more than 15000 h (continuous operation) was announced by MEA production company Danish Power Systems (now Blue World Technologies) [172]. However, the lifetime of HT-PEMFC stacks in integrated systems and in real-world applications could be much shorter due to the compounding of the degradation of different system components, especially due to composition and quality change of feed gases because of changes in reformer operating conditions, frequent dynamic operations, heat management issues, cell imbalance or failure, etc.

Degradation of HT-PEMFCs typically consists of chemical degradation, mechanical degradation and thermal degradation, which have been explicitly analyzed in many reviews [34,148,173]. The high working temperature, low humidity and acidic working environment of HT-PEMFCs exacerbates the components degradation, such as Pt dissolution, migration and agglomeration, carbon support corrosion, etc. It is considered that the chemical degradation especially the catalyst degradation of Pt particle size increase on the cathode side and carbon support corrosion are the main degradation mechanisms during the long-term steady-state operation [148].

The durability and corresponding degradation rates of HT-PEMFCs were obtained through literature survey as shown in Fig. 15. As can be seen, compared with steady-state operation, dynamic operations of load changes/cycling, thermal cycling and start/stop cycling, which are common in real-world applications, led to high degradation rate at similar test duration. This is because dynamic operations can accelerate not only the chemical degradation of catalyst and membrane, but also the mechanical and the thermal degradation, thereby significantly reducing the durability of HT-PEMFCs [32,148]. The degrading effect of cyclic operation is seen to depend on the dwell time of the cycled parameter. For instance, in the case of load cycling, the shorter the periods are at which the current is held constant, the worse is the impact (interval of 15 s) as shown in Fig. 15. Moçotéguy et al. [174,175] reported that cycling between 0.2 A cm^{-2} and 0.4 A cm^{-2} with dwell time of 12 h increases the degradation by a factor of 1.5 and dwell time of 6 h

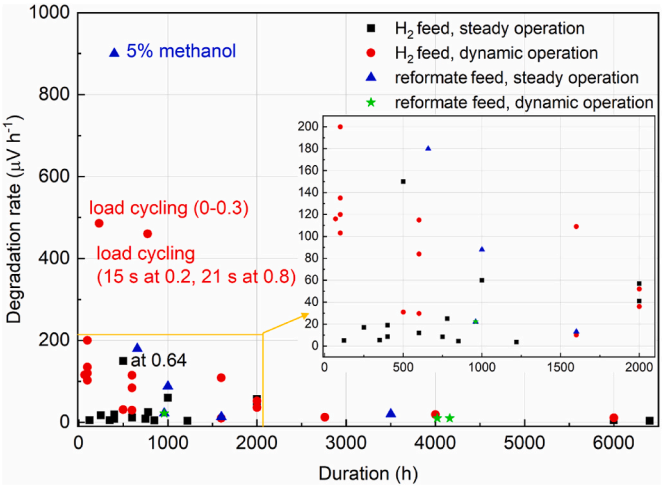

Fig. 15. Durability and the corresponding degradation rates of HT-PEMFC under different operating conditions from the literature (load units in the figure are A cm^{-2}).

leads to 4 times higher voltage decay. The authors also investigated the effect of a start/stop strategy and found that for 12 h cycling, the degradation doubled compared to continuous load, i.e., more than when cycling between 0.2 A cm^{-2} and 0.4 A cm^{-2} with a dwell time of 12 h. This could be due to potential open circuit voltage (OCV) operation during the start/stop cycling, which can exacerbate the degradation. For LT-PEMFCs, Borup et al. [176] investigated whether the number of cycles or the time at high potentials is crucial for voltage degradation due to cycling. They carried out an experiment at 80 °C where two cells were subject to potential cycling between 0.1 V and 0.96 V with a sweep rate of 10 mV/s and 50 mV/s, respectively, and found that the loss of the electrochemical surface area (ECSA) is comparable for both after six cycles, although the time at potentials over 0.9 V is very different. Since LT-PEMFC and HT-PEMFC have similar degradation mechanisms, it could be that the number of cycles may have greater impact on the degradation than the time at high potentials, even in the case of HT-PEMFCs.

Furthermore, with the development of HT-PEMFC technology, the performance of MEA has been improved. It has been reported by A. Kannan et al. [177,178] that the long-term stability of more than 4020 h operation (1562 cycles start-stop) only led to a degradation rate of 10.1 μV h^{-1} (the green dots around 4000 h in Fig. 15). In addition to the advancement in material of the components and system design, it is also necessary to implement good temperature and load control strategies in the system which can satisfy the required operation conditions and improve the system lifetime and durability.

On the reformer side, the deactivation of copper-based catalysts in the reformer that occurs during the MSR process is another challenge for the MSR-HT PEMFC system, which can lead to the loss of active site concentrations, which leads to the decrease in hydrogen yield, and the reduced selectivity toward hydrogen in the reformate gas [179]. The main causes of the catalyst deactivation include sintering, coking and physical damages. Catalyst deactivation could also occur when impurities (e.g., sulfur and chloride) are present in the feed [180–182]. Both sulfur- and chlorine-containing compounds can originate in feedstock during the methanol manufacturing process or be introduced during storage and transport [182].

Moreover, since MSR is a strongly endothermic process that requires external heat supplied to the reformer and it is difficult to properly control the temperature in the catalyst bed, catalyst overheating (>300 °C) may occur during the process (especially for dynamic operations), for instance, when an enormous amount of heat is supplied at lower reactant flow rates, resulting in the sintering of copper crystallites and irreversible loss of activity [183]. Coking deactivates the catalyst by forming carbonaceous deposits within the pore system and blocks the catalytic sites. Additionally, physical damages of copper-based catalysts, such as catalyst break-up due to vibration and temperature cycling, may also occur. The contribution of this factor to the catalyst deactivation is usually minimal compared to the above-mentioned more significant ones [182], but may need more investigations if the MSR process is under the operating conditions of automotive, marine and portable applications [179].

The system efficiency is also a key performance index (KPI), which involves product design and optimization at both system and components levels. For the MSR-HT-PEMFC system, the net electric efficiency was reported to be 41% for the 5 kW unit (by Advent) for stationary application [184]. If the heat produced in the system is further recovered, for instance, a CHP system for residential use, the overall system efficiency can reach up to 87% for a 1 kWe micro-CHP system [114]. With respect to the automotive applications, there could be challenges in some aspects of heat management and control strategy, due to frequent dynamic operations, such as dynamic load changes in the scenario of passenger vehicles [185]. However, these issues can be solved if a FC-battery hybrid system is used, where the battery takes the dynamic load changes and the fuel cell covers the constant base-load with only few preset load changes at longer load dwell times. Moreover, exergoeconomic analysis and machine-learning could be explored to further optimize the efficiency of such a system with multiple energy systems, where thermodynamic, economic and environmental performance is evaluated, and machine-learning algorithm is used to automate the system optimization process [186,187]. An example of an exergoeconomic machine-learning method for optimizing energy systems integration can be found in Ref. [188].

Another KPI is the system cost, which could include the costs of methanol reformer, fuel cell system (HT-PEMFC), power electronics, installation, sales markup and other possible costs [189]. The total share for the MSR-HT-PEMFC system is relatively small for CHP applications, e.g., around 25% (1566.8 $/kW) in the scenario of high manufacturing volume (5 kW, 50000 systems per year), due to the significant cost of installation for gas and electrical connection to the building (2506.8 $/kW), sales markup (1279.2 $/kW), power electronics (564.0 $/kW), and other possible parts (427.7 $/kW) [189]. For automotive applications, there is no additional installation cost compared to CHP application, and there should be less share for the sales markup, which can result in a higher share for the MSR-HT-PEMFC system, e.g., this share increases to around 36% and 55% for the conditions with and without sales markup, respectively, 25 kW, 50000 systems per year [189]. Compared with a LT-PEMFC system, the cost for a HT-PEMFC system is higher due to the lower power density (requiring larger stack) and higher loading of Pt catalyst per unit active area of fuel cell stacks [170,189], which necessitates the improvement and development of low-cost HT-PEMFC stack in future market.

In the future energy scenarios, the higher shares of intermittent renewable energy sources, such as the target of 32% (2030) by EU [190], will bring significant challenge in balancing the electrical grid. Power-to-X technologies provide possible solutions for this issue, where "X" can represent different pathways and energy carriers for storage and utilization of the surplus renewable electricity. Power-to-Methanol, also reported as part of the carbon-neutral methanol economy [161], is one pathway that shows great potential, where e-methanol is synthesized by green hydrogen (electrolysis based on renewable electricity) and CO_2 from biomass or carbon capture [191]. With respect to the consumption of e-methanol, the possible applications of the MSR-HT-PEMFC systems play important role in the value chain of the methanol economy, which can involve the industries and end users in the energy and transportation sectors and contribute to the green transition towards a climate-neutral economy by acting as enabler for PtX technologies.

7. Conclusion

In this paper, an overview of the MSR-HT-PEMFC systems was carried out, including the potential of methanol, which is considered a promising alternative to hydrogen as fuel for the MSR-HT-PEMFC systems. Compared to LT-PEMFC, HT-PEMFC is believed to be more suitable to integrate with MSR system due to its better water and thermal management and higher CO tolerance. The different working temperature of methanol reformer and HT-PEMFC leads to the low thermal and energy efficiency of the integrated MSR-HT-PEMFC system. The challenges and optimization of the MSR-HT-PEMFC system were thoroughly reviewed in this paper. A deep discussion of different kinds of reformer designs for the performance optimization of the corresponding reformer types and analysis of advantages and disadvantages of different integration methods and advances for the MSR-HT-PEMFC system integration are also provided. Besides, the dynamics of the MSR-HT-PEMFC system during application were discussed, based on which the control and diagnosis methods were discussed. Furthermore, the application, challenges and the advances, which considered the lifetime, efficiency and cost for the future commercial applications of the MSR-HT-PEMFC system, were elaborated.

For large scale market deployment, improvements in the following steps should still be further investigated: (1) the long startup time of the MSR-HT-PEMFC system should be addressed; (2) A more compact

structural design without sacrificing performance should be explored. In this regard, a water recovery in the system, where the water produce by fuel cell is used to satisfy the water need for MSR, can reduce the fuel tank size; (3) The design of the reformer should consider both the heat transfer and the pressure drop to maximize the system performance; (4) For catalyst of HT-PEMFC, development on higher temperature and impurity tolerance are necessary. Moreover, proton exchange membranes that can operate in the temperature range between 200 °C and 300 °C could be further carried out, which can allow better heat integration with the reformer. For reformer, studies on lower temperature tolerance without sacrificing conversion efficiency should be investigated for decreasing the temperature difference between the fuel cell and the reformer in the MSR-HT-PEMFC system; (5) More work should be done to increase durability and decrease the cost of components materials of the MSR-HT-PEMFC system. (6) Control and diagnostic methods should be further improved to enhance the durability and lifetime evaluation of the MSR-HT-PEMFC system.

Funding

This work was supported by Danish Energy Technology Development and Demonstration on Program (EUDP) through the MFC MultiGen project [grant number 64020–2073] and the BlueDolphin project [grant number 64021–2065].

Declaration of competing interest

The authors declare that they have no known competing financial interests or personal relationships that could have appeared to influence the work reported in this paper.

Data availability

No data was used for the research described in the article.

References

[1] International Energy Agency. Global energy review 2021. Global Energy Review 2020;2021:1–36.
[2] Defying expectations, CO2 emissions from global fossil fuel combustion are set to grow in 2022 by only a fraction of last year's big increase - News - IEA n.d. https://www.iea.org/news/defying-expectations-co2-emissions-from-global-fossil-fuel-combustion-are-set-to-grow-in-2022-by-only-a-fraction-of-last-year-s-big-increase (accessed February 16, 2023).
[3] Shafiee S, Topal E. When will fossil fuel reserves be diminished? Energy Pol 2009;37:181–9. https://doi.org/10.1016/j.enpol.2008.08.016.
[4] Global Overview n.d. https://www.ren21.net/gsr-2021/chapters/chapter_01/chapter_01/(accessed December 7, 2022).
[5] Gielen D, Boshell F, Saygin D, Bazilian MD, Wagner N, Gorini R. The role of renewable energy in the global energy transformation. Energy Strategy Rev 2019;24:38–50. https://doi.org/10.1016/j.esr.2019.01.006.
[6] Goldmann A, Sauter W, Oettinger M, Kluge T, Schröder U, Seume JR, et al. A study on electrofuels in aviation. Energies (Basel) 2018;11:1–23. https://doi.org/10.3390/en11020392.
[7] Herdem MS, Sinaki MY, Farhad S, Hamdullahpur F. An overview of the methanol reforming process: Comparison of fuels, catalysts, reformers, and systems. Int J Energy Res 2019;43:5076–105. https://doi.org/10.1002/er.4440.
[8] Yue M, Lambert H, Pahon E, Roche R, Jemei S, Hissel D. Hydrogen energy systems: a critical review of technologies, applications, trends and challenges. Renew Sustain Energy Rev 2021;146:111180. https://doi.org/10.1016/j.rser.2021.111180.
[9] Araya SS, Liso V, Cui X, Li N, Zhu J, Sahlin SL, et al. A review of the methanol economy: the fuel cell route. Energies (Basel) 2020;13. https://doi.org/10.3390/en13030596.
[10] Sarabchi N, Yari M, Mahmoudi SMS. Exergy and exergoeconomic analyses of novel high-temperature proton exchange membrane fuel cell based combined cogeneration cycles, including methanol steam reformer integrated with catalytic combustor or parabolic trough solar collector. J Power Sources 2021:485. https://doi.org/10.1016/j.jpowsour.2020.229277.
[11] Horng RF, Chou HM, Lee CH, Tsai H Te. Characteristics of hydrogen produced by partial oxidation and auto-thermal reforming in a small methanol reformer. J Power Sources 2006;161:1225–33. https://doi.org/10.1016/j.jpowsour.2006.06.043.
[12] Xing S, Zhao C, Ban S, Su H, Chen M, Wang H. A hybrid fuel cell system integrated with methanol steam reformer and methanation reactor. Int J Hydrogen Energy 2021;46:2565–76. https://doi.org/10.1016/j.ijhydene.2020.10.107.
[13] O'Hayre R, Cha S-W, Colella W, Prinz FB. Fuel cell fundamentals. Fuel Cell Fundamentals; 2016. https://doi.org/10.1002/9781119191766.
[14] Zhang S, Zhang Y, Chen J, Yin C, Liu X. Design, fabrication and performance evaluation of an integrated reformed methanol fuel cell for portable use. J Power Sources 2018;389:37–49. https://doi.org/10.1016/j.jpowsour.2018.04.009.
[15] The 4th Generation - Life Cycle Emissions of Hydrogen n.d. https://4thgeneration.energy/life-cycles-emissions-of-hydrogen/(accessed December 7, 2022).
[16] Bepari S, Kuila D. ScienceDirect Steam reforming of methanol , ethanol and glycerol over nickel-based catalysts-A review. Int J Hydrogen Energy 2019;45:18090–113. https://doi.org/10.1016/j.ijhydene.2019.08.003.
[17] Dalena F, Senatore A, Marino A, Gordano A, Basile M, Basile A. Methanol production and applications : an overview. Elsevier B.V.; 2018. https://doi.org/10.1016/B978-0-444-63903-5.00001-7.
[18] Araya SS, Grigoras IF, Zhou F, Andreasen SJ, Kær SK. Performance and endurance of a high temperature PEM fuel cell operated on methanol reformate. Int J Hydrogen Energy 2014;39:18343–50. https://doi.org/10.1016/j.ijhydene.2014.09.007.
[19] Papavasiliou J, Avgouropoulos G, Ioannides T. CuMnOx catalysts for internal reforming methanol fuel cells: application aspects. Int J Hydrogen Energy 2012;37. https://doi.org/10.1016/j.ijhydene.2012.02.124. 16739–47.
[20] Radenahmad N, Afif A, Petra PI, Rahman SMH, Eriksson SG, Azad AK. Proton-conducting electrolytes for direct methanol and direct urea fuel cells – a state-of-the-art review. Renew Sustain Energy Rev 2016;57:1347–58. https://doi.org/10.1016/J.RSER.2015.12.103.
[21] Bonenkamp TB, Middelburg LM, Hosli MO, Wolffenbuttel RF. From bioethanol containing fuels towards a fuel economy that includes methanol derived from renewable sources and the impact on European Union decision-making on transition pathways. Renew Sustain Energy Rev 2020;120:109667. https://doi.org/10.1016/J.RSER.2019.109667.
[22] Verhelst S, Turner JW, Sileghem L, Vancoillie J. Methanol as a fuel for internal combustion engines. Prog Energy Combust Sci 2019;70:43–88. https://doi.org/10.1016/J.PECS.2018.10.001.
[23] Tian X, Yang L, Gao R. Dynamic modeling and simulation of reformed methanol fuel cell system using Modelica. In: Proceedings of Asian Modelica conference 2020, vol. 174; 2020. p. 85–91. https://doi.org/10.3384/ecp202017485. Tokyo, Japan, October 08-09, 2020.
[24] Thomas S, Araya SS, Vang JR, Kær SK. Investigating different break-in procedures for reformed methanol high temperature proton exchange membrane fuel cells. Int J Hydrogen Energy 2018;43:14691–700. https://doi.org/10.1016/j.ijhydene.2018.05.166.
[25] Thomas S, Vang JR, Araya SS, Kær SK. Experimental study to distinguish the effects of methanol slip and water vapour on a high temperature PEM fuel cell at different operating conditions. Appl Energy 2017;192:422–36. https://doi.org/10.1016/j.apenergy.2016.11.063.
[26] Papavasiliou J, Avgouropoulos G, Ioannides T. CuMnOx catalysts for internal reforming methanol fuel cells: application aspects. Int J Hydrogen Energy 2012;37:16739–47. https://doi.org/10.1016/j.ijhydene.2012.02.124.
[27] Avgouropoulos G, Neophytides SG. Performance of internal reforming methanol fuel cell under various methanol/water concentrations. J Appl Electrochem 2012;42:719–26. https://doi.org/10.1007/s10800-012-0453-x.
[28] Ribeirinha P, Schuller G, Boaventura M, Mendes A. Synergetic integration of a methanol steam reforming cell with a high temperature polymer electrolyte fuel cell. Int J Hydrogen Energy 2017;42:13902–12. https://doi.org/10.1016/j.ijhydene.2017.01.172.
[29] Raza R, Akram N, Javed MS, Rafique A, Ullah K, Ali A, et al. Fuel cell technology for sustainable development in Pakistan - an over-view. Renew Sustain Energy Rev 2016;53:450–61. https://doi.org/10.1016/j.rser.2015.08.049.
[30] Ni M, Leung MK, DYC Leung, Sumathy K, Meng N. Prospect of proton exchange membrane fuel cells (PEMFC) for transportation flexible metal-air batteries view project microfluidics-based energy conversion reactor view project prospect of proton exchange membrane fuel cells (PEMFC) for transportation. ResearchGate [n.d].
[31] Wang Y, Seo B, Wang B, Zamel N, Jiao K, Adroher XC. Fundamentals, materials, and machine learning of polymer electrolyte membrane fuel cell technology. Energy AI 2020;1:100014. https://doi.org/10.1016/j.egyai.2020.100014.
[32] Rosli RE, Sulong AB, Daud WRW, Zulkifley MA, Husaini T, Rosli MI, et al. A review of high-temperature proton exchange membrane fuel cell (HT-PEMFC) system. Int J Hydrogen Energy 2017;42:9293–314. https://doi.org/10.1016/j.ijhydene.2016.06.211.
[33] Bose S, Kuila T, Nguyen TXH, Kim NH, Lau KT, Lee JH. Polymer membranes for high temperature proton exchange membrane fuel cell: recent advances and challenges. Prog Polym Sci (Oxford) 2011;36:813–43. https://doi.org/10.1016/j.progpolymsci.2011.01.003.
[34] Chandan A, Hattenberger M, El-Kharouf A, Du S, Dhir A, Self V, et al. High temperature (HT) polymer electrolyte membrane fuel cells (PEMFC)-A review. J Power Sources 2013;231:264–78. https://doi.org/10.1016/j.jpowsour.2012.11.126.
[35] Zamel N, Li X. Transient analysis of carbon monoxide poisoning and oxygen bleeding in a PEM fuel cell anode catalyst layer. Int J Hydrogen Energy 2008;33:1335–44. https://doi.org/10.1016/j.ijhydene.2007.12.060.
[36] Jiang R, Russell Kunz H, Fenton JM. Influence of temperature and relative humidity on performance and CO tolerance of PEM fuel cells with Nafion®-

Teflon®-Zr(HPO4)2 higher temperature composite membranes. Electrochim Acta 2006;51:5596–605. https://doi.org/10.1016/j.electacta.2006.02.033.
[37] Sun X, Simonsen SC, Norby T, Chatzitakis A. Composite membranes for high temperature PEM fuel cells and electrolysers: a critical review. Membranes (Basel) 2019;9. https://doi.org/10.3390/membranes9070083.
[38] Tahrim AA, Amin INHM. Advancement in phosphoric acid doped polybenzimidazole membrane for high temperature PEM fuel cells: a review. J Appl Membr Sci Technol 2018;23:37–62. https://doi.org/10.11113/amst.v23n1.136.
[39] Li Q, He R, Gao J-A, Jensen JO, Bjerrum NielsJ. The CO poisoning effect in PEMFCs operational at temperatures up to 200°C. J Electrochem Soc 2003;150:A1599. https://doi.org/10.1149/1.1619984.
[40] Asensio JA, Sánchez EM, Romero PG. Proton-conducting membranes based on benzimidazole polymers for high-temperature PEM fuel cells. A chemical quest. Chem Soc Rev 2010;39:3210–39. https://doi.org/10.1039/b922650h.
[41] Araya SS, Zhou F, Liso V, Sahlin SL, Vang JR, Thomas S, et al. A comprehensive review of PBI-based high temperature PEM fuel cells. Int J Hydrogen Energy 2016;41:21310–44. https://doi.org/10.1016/j.ijhydene.2016.09.024.
[42] Zhang J, Xie Z, Zhang J, Tang Y, Song C, Navessin T, et al. High temperature PEM fuel cells. J Power Sources 2006;160:872–91. https://doi.org/10.1016/j.jpowsour.2006.05.034.
[43] Gang X, Qingfeng L, Hjuler HA, Bjerrum NJ. Hydrogen oxidation on gas diffusion electrodes for phosphoric acid fuel cells in the presence of carbon monoxide and oxygen. J Electrochem Soc 1995;142:2890–3. https://doi.org/10.1149/1.2048660.
[44] Jeppesen C, Polverino P, Andreasen SJ, Araya SS, Sahlin SL, Pianese C, et al. Impedance characterization of high temperature proton exchange membrane fuel cell stack under the influence of carbon monoxide and methanol vapor. Int J Hydrogen Energy 2017;42. https://doi.org/10.1016/j.ijhydene.2017.07.094. 21901–12.
[45] Thomas S, Vang JR, Araya SS, Kær SK. Experimental study to distinguish the effects of methanol slip and water vapour on a high temperature PEM fuel cell at different operating conditions. Appl Energy 2017;192:422–36. https://doi.org/10.1016/j.apenergy.2016.11.063.
[46] Kvesić M, Reimer U, Froning D, Lüke L, Lehnert W, Stolten D. 3D modeling of an HT-PEFC stack using reformate gas. Int J Hydrogen Energy 2012;37:12438–50. https://doi.org/10.1016/j.ijhydene.2012.05.113.
[47] Sahlin SL, Andreasen SJ, Kær SK. System model development for a methanol reformed 5 kW high temperature PEM fuel cell system. Int J Hydrogen Energy 2015;40:13080–9. https://doi.org/10.1016/j.ijhydene.2015.07.145.
[48] Lang S, Kazdal TJ, Kühl F, Hampe MJ. Experimental investigation and numerical simulation of the electrolyte loss in a HT-PEM fuel cell. Int J Hydrogen Energy 2015;40:1163–72. https://doi.org/10.1016/j.ijhydene.2014.11.041.
[49] Reimer U, Ehlert J, Janßen H, Lehnert W. Water distribution in high temperature polymer electrolyte fuel cells. Int J Hydrogen Energy 2016;41:1837–45. https://doi.org/10.1016/j.ijhydene.2015.11.106.
[50] Nguyen G, Sahlin S, Andreasen SJ, Shaffer B, Brouwer J. Dynamic modeling and experimental investigation of a high temperature PEM fuel cell stack. Int J Hydrogen Energy 2016;41:4729–39. https://doi.org/10.1016/j.ijhydene.2016.01.045.
[51] Weiß A, Schindler S, Galbiati S, Danzer MA, Zeis R. Distribution of relaxation times analysis of high-temperature PEM fuel cell impedance spectra. Electrochim Acta 2017;230:391–8. https://doi.org/10.1016/j.electacta.2017.02.011.
[52] Ribeirinha P, Abdollahzadeh M, Pereira A, Relvas F, Boaventura M, Mendes A. High temperature PEM fuel cell integrated with a cellular membrane methanol steam reformer: experimental and modelling. Appl Energy 2018;215:659–69. https://doi.org/10.1016/j.apenergy.2018.02.029.
[53] Ribeirinha P, Schuller G, Boaventura M, Mendes A. Synergetic integration of a methanol steam reforming cell with a high temperature polymer electrolyte fuel cell. Int J Hydrogen Energy 2017;42:13902–12. https://doi.org/10.1016/j.ijhydene.2017.01.172.
[54] Drakselová M, Kodým R, Šnita D, Beckmann F, Bouzek K. Three-dimensional macrohomogeneous mathematical model of an industrial-scale high-temperature PEM fuel cell stack. Electrochim Acta 2018;273:432–46. https://doi.org/10.1016/j.electacta.2018.04.042.
[55] Bandlamudi V, Bujlo P, Linkov V, Pasupathi S. The effect of potential cycling on high temperature PEM fuel cell with different flow field designs. Fuel Cell 2019;19:231–43. https://doi.org/10.1002/fuce.201800127.
[56] Yao Tian X, Lin Yang L, Gao R. Dynamic Modeling and Simulation of Reformed methanol Fuel Cell System Using Modelica n.d. https://doi.org/10.3384/ecp2017485.
[57] Sun Z, Sun Z qiang. Hydrogen generation from methanol reforming for fuel cell applications: a review. J Cent South Univ 2020;27:1074–103. https://doi.org/10.1007/s11771-020-4352-8.
[58] Zhao J, Shi R, Li Z, Zhou C, Zhang T. How to make use of methanol in green catalytic hydrogen production? Nano Select 2020;1:12–29. https://doi.org/10.1002/nano.202000010.
[59] Li H, Ma C, Zou X, Li A, Huang Z, Zhu L. On-board methanol catalytic reforming for hydrogen Production-A review. Int J Hydrogen Energy 2021;46:22303–27. https://doi.org/10.1016/j.ijhydene.2021.04.062.
[60] Xu X, Shuai K, Xu B. Review on copper and palladium based catalysts for methanol steam reforming to produce hydrogen. Catalysts 2017;7. https://doi.org/10.3390/catal7060183.
[61] Chougule A, Sonde RR. Modelling and experimental investigation of compact packed bed design of methanol steam reformer. Int J Hydrogen Energy 2019;44:29937–45. https://doi.org/10.1016/j.ijhydene.2019.09.166.
[62] Nehe P, Reddy VM, Kumar S. ScienceDirect Investigations on a new internally-heated tubular packed-bed methanol e steam reformer. Int J Hydrogen Energy 2015;40:5715–25. https://doi.org/10.1016/j.ijhydene.2015.02.114.
[63] Sanz O, Velasco I, Pérez-Miqueo I, Poyato R, Odriozola JA, Montes M. Intensification of hydrogen production by methanol steam reforming. Int J Hydrogen Energy 2016;41:5250–9. https://doi.org/10.1016/j.ijhydene.2016.01.084.
[64] Andreasen SJ, Kær SK, Sahlin S. Control and experimental characterization of a methanol reformer for a 350 W high temperature polymer electrolyte membrane fuel cell system. Int J Hydrogen Energy 2013;38:1676–84. https://doi.org/10.1016/j.ijhydene.2012.09.032.
[65] Justesen KK, Andreasen SJ. Determination of optimal reformer temperature in a reformed methanol fuel cell system using ANFIS models and numerical optimization methods. Int J Hydrogen Energy 2015;40:9505–14. https://doi.org/10.1016/j.ijhydene.2015.05.085.
[66] Araya SS, Grigoras IF, Zhou F, Andreasen SJ, Kær SK. Performance and endurance of a high temperature PEM fuel cell operated on methanol reformate. Int J Hydrogen Energy 2014;39:18343–50. https://doi.org/10.1016/j.ijhydene.2014.09.007.
[67] Wang Y, Ruiz Diaz DF, Chen KS, Wang Z, Adroher XC. Materials, technological status, and fundamentals of PEM fuel cells – a review. Mater Today 2020;32:178–203. https://doi.org/10.1016/j.mattod.2019.06.005.
[68] Schuller G, Vázquez FV, Waiblinger W, Auvinen S, Ribeirinha P. Heat and fuel coupled operation of a high temperature polymer electrolyte fuel cell with a heat exchanger methanol steam reformer. J Power Sources 2017;347:47–56. https://doi.org/10.1016/j.jpowsour.2017.02.021.
[69] Herdem MS, Sinaki MY, Farhad S, Hamdullahpur F. An overview of the methanol reforming process: Comparison of fuels, catalysts, reformers, and systems. Int J Energy Res 2019;43:5076–105. https://doi.org/10.1002/er.4440.
[70] Ribeirinha P, Alves I, Vázquez FV, Schuller G, Boaventura M, Mendes A. Heat integration of methanol steam reformer with a high-temperature polymeric electrolyte membrane fuel cell. Energy 2017;120:468–77. https://doi.org/10.1016/j.energy.2016.11.101.
[71] Herdem MS, Sinaki MY, Farhad S, Hamdullahpur F. An overview of the methanol reforming process: Comparison of fuels, catalysts, reformers, and systems. Int J Energy Res 2019;43:5076–105. https://doi.org/10.1002/er.4440.
[72] Peppley BA, Amphlett JC, Kearns LM, Mann RF. Methanol-steam reforming on Cu/ZnO/Al2O3 catalysts. Part 2. A comprehensive kinetic model. Appl Catal Gen 1999;179:31–49. https://doi.org/10.1016/S0926-860X(98)00299-3.
[73] Thattarathody R, Sheintuch M. Kinetics and dynamics of methanol steam reforming on CuO/ZnO/alumina catalyst. Appl Catal Gen 2017;540:47–56. https://doi.org/10.1016/j.apcata.2017.04.012.
[74] Liao CH, Horng RF. Investigation on the hydrogen production by methanol steam reforming with engine exhaust heat recovery strategy. Int J Hydrogen Energy 2016;41:4957–68. https://doi.org/10.1016/j.ijhydene.2016.01.100.
[75] Ribeirinha P, Abdollahzadeh M, Sousa JM, Boaventura M, Mendes A. Modelling of a high-temperature polymer electrolyte membrane fuel cell integrated with a methanol steam reformer cell. Appl Energy 2017;202:6–19. https://doi.org/10.1016/j.apenergy.2017.05.120.
[76] Sari A, Sabziani J. Modeling and 3D-simulation of hydrogen production via methanol steam reforming in copper-coated channels of a mini reformer. J Power Sources 2017;352:64–76. https://doi.org/10.1016/j.jpowsour.2017.03.120.
[77] Wang F, Li L, Liu Y. Effects of flow and operation parameters on methanol steam reforming in tube reactor heated by simulated waste heat. Int J Hydrogen Energy 2017;42:26270–6. https://doi.org/10.1016/j.ijhydene.2017.09.002.
[78] Chiu YJ, Chiu HC, Hsieh RH, Jang JH, Jiang BY. Simulations of hydrogen production by methanol steam reforming. Energy Proc 2019;156:38–42. https://doi.org/10.1016/j.egypro.2018.11.081.
[79] Özcan O, Akın AN. Thermodynamic analysis of methanol steam reforming to produce hydrogen for HT-PEMFC: an optimization study. Int J Hydrogen Energy 2019;44:14117–26. https://doi.org/10.1016/j.ijhydene.2018.12.211.
[80] Gurau V, Ogunleke A, Strickland F. Design of a methanol reformer for on-board production of hydrogen as fuel for a 3 kW High-Temperature Proton Exchange Membrane Fuel Cell power system. Int J Hydrogen Energy 2020;45:31745–59. https://doi.org/10.1016/j.ijhydene.2020.08.179.
[81] Xing S, Zhao C, Ban S, Liu Y, Wang H. Thermodynamic performance analysis of the influence of multi-factor coupling on the methanol steam reforming reaction. Int J Hydrogen Energy 2020;45:7015–24. https://doi.org/10.1016/j.ijhydene.2019.12.192.
[82] Zhuang X, Xu X, Li L, Deng D. Numerical investigation of a multichannel reactor for syngas production by methanol steam reforming at various operating conditions. Int J Hydrogen Energy 2020;45:14790–805. https://doi.org/10.1016/j.ijhydene.2020.03.207.
[83] Zhuang X, Xia X, Xu X, Li L. Experimental investigation on hydrogen production by methanol steam reforming in a novel multichannel micro packed bed reformer. Int J Hydrogen Energy 2020;45:11024–34. https://doi.org/10.1016/j.ijhydene.2020.02.034.
[84] Wang Y, Wu Q, Mei D, Wang Y. A methanol fuel processing system with methanol steam reforming and CO selective methanation modules for PEMFC application. Int J Energy Res 2021;45:6163–73. https://doi.org/10.1002/er.6239.
[85] Zhu J, Araya SS, Cui X, Sahlin SL, Kær SK. Modeling and design of a multi-tubular packed-bed reactor for methanol steam reforming over a Cu/ZnO/Al2O3 catalyst. Energies (Basel) 2020;13. https://doi.org/10.3390/en13030610.
[86] Karim A, Bravo J, Gorm D, Conant T, Datye A. Comparison of wall-coated and packed-bed reactors for steam reforming of methanol. Catal Today 2005;110:86–91. https://doi.org/10.1016/j.cattod.2005.09.010.

[87] Ribeirinha P, Boaventura M, Lopes JCB, Sousa JM, Mendes A. Study of different designs of methanol steam reformers: experiment and modeling. Int J Hydrogen Energy 2014;39:19970–81. https://doi.org/10.1016/j.ijhydene.2014.10.029.
[88] Wang HHF, Chen SC, Yang SY, Yeh GT, Rei MH. Design of compact methanol reformer for hydrogen with low CO for the fuel cell power generation. Int J Hydrogen Energy 2012;37:7487–96. https://doi.org/10.1016/j.ijhydene.2012.01.100.
[89] Ji F, Yang L, Li Y, Sun H, Sun G. Performance enhancement by optimizing the reformer for an internal reforming methanol fuel cell. Energy Sci Eng 2019;7:2814–24. https://doi.org/10.1002/ese3.461.
[90] Nehe P, Reddy VM, Kumar S. Investigations on a new internally-heated tubular packed-bed methanol-steam reformer. Int J Hydrogen Energy 2015;40:5715–25. https://doi.org/10.1016/j.ijhydene.2015.02.114.
[91] Perng SW, Horng RF, Wu HW. Effect of a diffuser on performance enhancement of a cylindrical methanol steam reformer by computational fluid dynamic analysis. Appl Energy 2017;206:312–28. https://doi.org/10.1016/j.apenergy.2017.08.194.
[92] Hao Y, Du X, Yang L, Shen Y, Yang Y. Numerical simulation of configuration and catalyst-layer effects on micro-channel steam reforming of methanol. Int J Hydrogen Energy 2011;36:15611–21. https://doi.org/10.1016/j.ijhydene.2011.09.038.
[93] Ryi SK, Park JS, Choi SH, Cho SH, Kim SH. Novel micro fuel processor for PEMFCs with heat generation by catalytic combustion. Chem Eng J 2005;113:47–53. https://doi.org/10.1016/j.cej.2005.08.008.
[94] Perng SW, Wu HW. Effect of depth and diameter of cylindrical cavity in a plate-type methanol steam reformer on estimated net power of PEMFC. Energy Convers Manag 2018;177:190–209. https://doi.org/10.1016/j.enconman.2018.09.066.
[95] Bravo J, Karim A, Conant T, Lopez GP, Datye A. Wall coating of a CuO/ZnO/Al2O3 methanol steam reforming catalyst for micro-channel reformers. Chem Eng J 2004;101:113–21. https://doi.org/10.1016/j.cej.2004.01.011.
[96] Lee M tsang, Greif R, Grigoropoulos CP, Park HG, Hsu FK. Transport in packed-bed and wall-coated steam-methanol reformers. J Power Sources 2007;166:194–201. https://doi.org/10.1016/j.jpowsour.2007.01.007.
[97] Chein RY, Chen LC, Chen YC, Chung JN. Heat transfer effects on the methanol-steam reforming with partially filled catalyst layers. Int J Hydrogen Energy 2009;34:5398–408. https://doi.org/10.1016/j.ijhydene.2009.04.049.
[98] Mahmoudizadeh M, Irankhah A, Irankhah R, Jafari M. Development of a replaceable microreactor coated with a CuZnFe nanocatalyst for methanol steam reforming. Chem Eng Technol 2016;39:322–30. https://doi.org/10.1002/ceat.201500101.
[99] Liguori S, Iulianelli A, Dalena F, Piemonte V, Huang Y, Basile A. Methanol steam reforming in an Al2O3supported thin Pd-layer membrane reactor over Cu/ZnO/Al2O3catalyst. Int J Hydrogen Energy 2014;39:18702. https://doi.org/10.1016/j.ijhydene.2013.11.113. –10.
[100] Chein RY, Chen YC, Chung JNC. Mathematical modeling of hydrogen production via methanol-steam reforming with heat-coupled and membrane-assisted reactors. Chem Eng Technol 2014;37:1907–18. https://doi.org/10.1002/ceat.201400224.
[101] Iulianelli A, Ghasemzadeh K, Basile A. Progress in methanol steam reforming modelling via membrane reactors technology. Membranes (Basel) 2018;8. https://doi.org/10.3390/membranes8030065.
[102] Miyamoto M, Hayakawa C, Kamata K, Arakawa M, Uemiya S. Influence of the pre-reformer in steam reforming of dodecane using a Pd alloy membrane reactor. Int J Hydrogen Energy 2011;36:7771–5. https://doi.org/10.1016/j.ijhydene.2011.01.089.
[103] Ribeirinha P, Abdollahzadeh M, Pereira A, Relvas F, Boaventura M, Mendes A. High temperature PEM fuel cell integrated with a cellular membrane methanol steam reformer: experimental and modelling. Appl Energy 2018;215:659–69. https://doi.org/10.1016/j.apenergy.2018.02.029.
[104] Park GG, Yim SD, Yoon YG, Kim CS, Seo DJ, Eguchi K. Hydrogen production with integrated microchannel fuel processor using methanol for portable fuel cell systems. Catal Today 2005;110:108–13. https://doi.org/10.1016/j.cattod.2005.09.016.
[105] Zhou W, Deng W, Lu L, Zhang J, Qin L, Ma S, et al. Laser micro-milling of microchannel on copper sheet as catalyst support used in microreactor for hydrogen production. Int J Hydrogen Energy 2014;39:4884–94. https://doi.org/10.1016/j.ijhydene.2014.01.041.
[106] Heidarzadeh M, Taghizadeh M. Methanol steam reforming in a spiral-shaped microchannel reactor over Cu/ZnO/Al2O3Catalyst: a computational fluid dynamics simulation study. Int J Chem React Eng 2017;15. https://doi.org/10.1515/ijcre-2016-0205.
[107] Lu W, Zhang R, Toan S, Xu R, Zhou F, Sun Z, et al. Microchannel structure design for hydrogen supply from methanol steam reforming. Chem Eng J 2022;429:132286. https://doi.org/10.1016/j.cej.2021.132286.
[108] Chen J, Li T, Meng F, Ming P. Characteristics of intraphase transport processes in methanol reforming microchannel reactors: a computational fluid dynamics study. Int J Hydrogen Energy 2020;45:17088–103. https://doi.org/10.1016/j.ijhydene.2020.04.128.
[109] Zhang S, Zhang Y, Chen J, Zhang X, Liu X. High yields of hydrogen production from methanol steam reforming with a cross-U type reactor. PLoS One 2017;12:1–14. https://doi.org/10.1371/journal.pone.0187802.
[110] Kang J, Song Y, Kim T, Kim S. Recent trends in the development of reactor systems for hydrogen production via methanol steam reforming. Int J Hydrogen Energy 2021;47:3587–610. https://doi.org/10.1016/j.ijhydene.2021.11.041.
[111] Kundu A, Park JM, Ahn JE, Park SS, Shul YG, Han HS. Micro-channel reactor for steam reforming of methanol. Fuel 2007;86:1331–6. https://doi.org/10.1016/j.fuel.2006.08.003.
[112] Yu D, Van NT, Yun J, Yu S. A thermal design of a 1kw-class shell and tube methanol steam reforming system with internal evaporator. Processes 2020;8:1–10. https://doi.org/10.3390/pr8111509.
[113] Herdem MS, Farhad S, Hamdullahpur F. Modeling and parametric study of a methanol reformate gas-fueled HT-PEMFC system for portable power generation applications. Energy Convers Manag 2015;101:19–29. https://doi.org/10.1016/j.enconman.2015.05.004.
[114] Wichmann D, Engelhardt P, Wruck R, Lucka K, Köhne H. Development of a highly integrated micro fuel processor based on methanol steam reforming for a HT-PEM fuel cell with an electric power output of 30 W. ECS Trans 2010;26:505–15. https://doi.org/10.1149/1.3429023.
[115] Romero-Pascual E, Soler J. Modelling of an HTPEM-based micro-combined heat and power fuel cell system with methanol. Int J Hydrogen Energy 2014;39:4053–9. https://doi.org/10.1016/J.IJHYDENE.2013.07.015.
[116] Lotrič A, Sekavčnik M, Pohar A, Likozar B, Hočevar S. Conceptual design of an integrated thermally self-sustained methanol steam reformer – high-temperature PEM fuel cell stack manportable power generator. Int J Hydrogen Energy 2017;42:16700–13. https://doi.org/10.1016/J.IJHYDENE.2017.05.057.
[117] Schuller G, Vázquez FV, Waiblinger W, Auvinen S, Ribeirinha P. Heat and fuel coupled operation of a high temperature polymer electrolyte fuel cell with a heat exchanger methanol steam reformer. J Power Sources 2017;347:47–56. https://doi.org/10.1016/j.jpowsour.2017.02.021.
[118] Ghodba A, Sharifzadeh M, Rashtchian D. Integrated and inherently safe design and operation of a mobile power generation: process intensification through microreactor reformer and HT-PEMFC. Int J Hydrogen Energy 2021;46:23839–54. https://doi.org/10.1016/J.IJHYDENE.2021.04.176.
[119] Liu J, Zhou Z, Yue B, Sun Z, Sun Z. Chemical looping induced CH3OH–H2-PEMFC scheme for fuel cell vehicle: parameter optimization and feasibility analysis. J Power Sources 2020;479:228790. https://doi.org/10.1016/J.JPOWSOUR.2020.228790.
[120] Avgouropoulos G, Neophytides SG. Performance of internal reforming methanol fuel cell under various methanol/water concentrations. J Appl Electrochem 2012;42:719–26. https://doi.org/10.1007/s10800-012-0453-x.
[121] Avgouropoulos G, Papavasiliou J, Daletou MK, Kallitsis JK, Ioannides T, Neophytides S. Reforming methanol to electricity in a high temperature PEM fuel cell. Appl Catal, B 2009;90:628–32. https://doi.org/10.1016/j.apcatb.2009.04.025.
[122] Papavasiliou J, Schütt C, Kolb G, Neophytides S, Avgouropoulos G. Technological aspects of an auxiliary power unit with internal reforming methanol fuel cell. Int J Hydrogen Energy 2019;44:12818–28. https://doi.org/10.1016/j.ijhydene.2018.11.136.
[123] Avgouropoulos G, Paxinou A, Neophytides S. In situ hydrogen utilization in an internal reforming methanol fuel cell. Elsevier Ltd Int J Hydrogen Energy 2014;39. https://doi.org/10.1016/j.ijhydene.2014.03.101. 18103–8.
[124] Avgouropoulos G, Papavasiliou J, Ioannides T, Neophytides S. Insights on the effective incorporation of a foam-based methanol reformer in a high temperature polymer electrolyte membrane fuel cell. J Power Sources 2015;296:335–43. https://doi.org/10.1016/j.jpowsour.2015.07.055.
[125] Park J, Min K. Dynamic modeling of a high-temperature proton exchange membrane fuel cell with a fuel processor. Int J Hydrogen Energy 2014;39:10683–96. https://doi.org/10.1016/j.ijhydene.2014.04.210.
[126] Avgouropoulos G, Papavasiliou J, Ioannides T, Neophytides S. Insights on the effective incorporation of a foam-based methanol reformer in a high temperature polymer electrolyte membrane fuel cell. J Power Sources 2015;296:335–43. https://doi.org/10.1016/j.jpowsour.2015.07.055.
[127] Avgouropoulos G, Paxinou A, Neophytides S. In situ hydrogen utilization in an internal reforming methanol fuel cell. Int J Hydrogen Energy 2014;39:18103–8. https://doi.org/10.1016/j.ijhydene.2014.03.101.
[128] Ribeirinha P, Abdollahzadeh M, Pereira A, Relvas F, Boaventura M, Mendes A. High temperature PEM fuel cell integrated with a cellular membrane methanol steam reformer: experimental and modelling. Appl Energy 2018;215:659–69. https://doi.org/10.1016/j.apenergy.2018.02.029.
[129] Weng F, Cheng CK, Chen KC. Hydrogen production of two-stage temperature steam reformer integrated with PBI membrane fuel cells to optimize thermal management. Int J Hydrogen Energy 2013;38:6059–64. https://doi.org/10.1016/j.ijhydene.2013.01.090.
[130] Wang J, Wu J, Xu Z, Li M. Thermodynamic performance analysis of a fuel cell trigeneration system integrated with solar-assisted methanol reforming. Energy Convers Manag 2017;150:81–9. https://doi.org/10.1016/j.enconman.2017.08.012.
[131] Ramaswamy S, Sundaresan M, Eggert A, Moore RM. System dynamics and efficiency of the fuel processor for an indirect methanol fuel cell vehicle. Institute of Electrical and Electronics Engineers (IEEE); 2002. p. 1372–7. https://doi.org/10.1109/iecec.2000.870953.
[132] Liang D, Shen Q, Hou M, Shao Z, Yi B. Study of the cell reversal process of large area proton exchange membrane fuel cells under fuel starvation. J Power Sources 2009;194:847–53. https://doi.org/10.1016/j.jpowsour.2009.06.059.
[133] Zhou F, Andreasen SJ, Kær SK, Yu D. Analysis of accelerated degradation of a HT-PEM fuel cell caused by cell reversal in fuel starvation condition. Int J Hydrogen Energy 2015;40:2833–9. https://doi.org/10.1016/j.ijhydene.2014.12.082.
[134] Zhang G, Kandlikar SG. A critical review of cooling techniques in proton exchange membrane fuel cell stacks. Int J Hydrogen Energy 2012;37:2412–29. https://doi.org/10.1016/j.ijhydene.2011.11.010.

[135] Bargal MHS, Abdelkareem MAA, Tao Q, Li J, Shi J, Wang Y. Liquid cooling techniques in proton exchange membrane fuel cell stacks: a detailed survey. Alex Eng J 2020;59:635–55. https://doi.org/10.1016/j.aej.2020.02.005.
[136] Kaer J, Sahlin SK, Justesen SL. Design and control of high temperature PEM fuel cell systems using methanol reformers with air or liquid heat integration: proceedings CD. 2013.
[137] Stamps AT, Gatzke EP. Dynamic modeling of a methanol reformer-PEMFC stack system for analysis and design. J Power Sources 2006;161:356–70. https://doi.org/10.1016/j.jpowsour.2006.04.080.
[138] Justesen KK, Andreasen SJ, Pasupathi S, Pollet BG. Modeling and control of the output current of a reformed methanol fuel cell system. Int J Hydrogen Energy 2015;40:16521–31. https://doi.org/10.1016/j.ijhydene.2015.10.006.
[139] Adinolfi EA, Gallo M, Polverino P, Beretta D, Araya SS, Pianese C. ECM-based algorithm for on-board PEMFCs diagnosis. Lecture Notes in Electrical Engineering 2020;697:103–15. https://doi.org/10.1007/978-3-030-56970-9_9. Springer Science and Business Media Deutschland GmbH.
[140] Andújar JM, Segura F, Isorna F, Calderón AJ. Comprehensive diagnosis methodology for faults detection and identification, and performance improvement of Air-Cooled Polymer Electrolyte Fuel Cells. Renew Sustain Energy Rev 2018;88:193–207. https://doi.org/10.1016/j.rser.2018.02.038.
[141] Polverino P, Pianese C. Model-based prognostic algorithm for online RUL estimation of PEMFCs. In: Conference on control and fault-tolerant systems, SysTol, vol. 2016. IEEE Computer Society; 2016. p. 599–604. https://doi.org/10.1109/SYSTOL.2016.7739814.
[142] Darowicki K, Janicka E, Mielniczek M, Zielinski A, Gawel L, Mitzel J, et al. Implementation of DEIS for reliable fault monitoring and detection in PEMFC single cells and stacks. Electrochim Acta 2018;292:383–9. https://doi.org/10.1016/j.electacta.2018.09.105.
[143] Dijoux E, Steiner NY, Benne M, Péra M-C, Pérez BG. A review of fault tolerant control strategies applied to proton exchange membrane fuel cell systems. J Power Sources 2017;359:119–33. https://doi.org/10.1016/J.JPOWSOUR.2017.05.058.
[144] Araya SS, Zhou F, Sahlin SL, Thomas S, Jeppesen C, Kær SK. Fault characterization of a proton exchange membrane fuel cell stack. Energies 2019;12:152. https://doi.org/10.3390/EN12010152. 2019;12:152.
[145] Real operation pem fuel cells HEALTH-state monitoring and diagnosis based on dc-dc COnverter embeddeD Eis;H2020, European project, Horizon 2020; Health-Code n.d. http://pemfc.health-code.eu/(accessed December 8, 2022).
[146] Jeppesen C, Araya SS, Sahlin SL, Andreasen SJ, Kær SK. An EIS alternative for impedance measurement of a high temperature PEM fuel cell stack based on current pulse injection. Int J Hydrogen Energy 2017. https://doi.org/10.1016/j.ijhydene.2017.05.066.
[147] Jeppesen C, Araya SS, Sahlin SL, Thomas S, Andreasen SJ, Kær SK. Fault detection and isolation of high temperature proton exchange membrane fuel cell stack under the influence of degradation. J Power Sources 2017;359:37–47. https://doi.org/10.1016/j.jpowsour.2017.05.021.
[148] Araya SS, Zhou F, Liso V, Sahlin SL, Vang JR, Thomas S, et al. A comprehensive review of PBI-based high temperature PEM fuel cells. Int J Hydrogen Energy 2016;41:21310–44. https://doi.org/10.1016/j.ijhydene.2016.09.024.
[149] Qingfeng L, Hjuler HA, Hasiotis C, Kallitsis JK, Kontoyannis CG, Bjerrum NJ. A quasi-direct methanol fuel cell system based on blend polymer membrane electrolytes. Electrochem Solid State Lett 2002;5:A125. https://doi.org/10.1149/1.1473335.
[150] Automotive - Advent Technologies n.d. https://www.advent.energy/automotive/(accessed December 5, 2022).
[151] Transportation-Palcan Energy Corporation n.d. http://www.palcan.com/transportation/(accessed December 5, 2022).
[152] Methanol fuel cell modules | SIQENS Ecoport n.d. https://siqens.de/en/fuel-cells/(accessed December 5, 2022).
[153] Automotive - Blue World Technologies n.d. https://www.blue.world/markets/automotive/(accessed December 5, 2022).
[154] IEA. Transport Improving the sustainability of passenger and freight transport n.d. https://www.iea.org/topics/transport.
[155] IEA. Hydrogen n.d. https://www.iea.org/reports/hydrogen.
[156] Tran M-K, Bhatti A, Vrolyk R, Wong D, Panchal S, Fowler M, et al. A review of range extenders in battery electric vehicles: current progress and future perspectives. World Electric Vehicle Journal 2021;12. https://doi.org/10.3390/wevj12020054.
[157] Liu Y, Lehnert W, Janßen H, Samsun RC, Stolten D. A review of high-temperature polymer electrolyte membrane fuel-cell (HT-PEMFC)-based auxiliary power units for diesel-powered road vehicles. J Power Sources 2016;311:91–102.
[158] Aalborg university. BlueDolphin; 2022. https://vbn.aau.dk/en/projects/bluedolphin.
[159] Commercial collaboration between Tuco Marine and Blue World Technologies - Blue World Technologies n.d https://www.blue.world/commercial-collaboration-between-tuco-marine-and-blue-world-technologies/(accessed June 9, 2022).
[160] EUDP. Marine fuel cell APU. 2021. https://eudp.dk/en/node/16075.
[161] Simon Araya S, Liso V, Cui X, Li N, Zhu J, Sahlin SL, et al. A review of the methanol economy: the fuel cell route. Energies (Basel) 2020;13:596. https://doi.org/10.3390/en13030596.
[162] Wilberforce T, Alaswad A, Palumbo A, Dassisti M, Olabi AG. Advances in stationary and portable fuel cell applications. Int J Hydrogen Energy 2016;41:16509–22. https://doi.org/10.1016/j.ijhydene.2016.02.057.
[163] Units - advent technologies. n.d, https://serene.advent.energy/units/. [Accessed 16 June 2022].
[164] Transportation-palcan energy corporation. n.d, http://www.palcan.com/transportation/. [Accessed 16 June 2022].
[165] Supplemental Power Generation | EUDP n.d. https://eudp.dk/projekter/supplemental-power-generation (accessed June 9, 2022).
[166] Cabinets - Advent Technologies n.d https://serene.advent.energy/cabinets/ (accessed July 7, 2022).
[167] EUDP. MFC MultiGen n.d. https://eudp.dk/projekter/mfc-multigen.
[168] European Union. EMPOWER - European methanol powered fuel cell CHP n.d. https://www.empower-euproject.eu/the-project/.
[169] Zhang J, Xie Z, Zhang J, Tang Y, Song C, Navessin T, et al. High temperature PEM fuel cells. J Power Sources 2006;160:872–91. https://doi.org/10.1016/j.jpowsour.2006.05.034.
[170] Wei M, Lipman T, Mayyas A, Chien J, Chan SH, Gosselin D, et al. A total cost of ownership model for low temperature PEM fuel cells in combined heat and power and backup power applications. Berkeley, CA (United States): Lawrence Berkeley National Lab.(LBNL); 2014.
[171] BASF. Proton-Conductive Membrane n.d https://www.basf.com/global/en/who-we-are/organization/group-companies/BASF_New-Business-GmbH/our-solutions/proton-conductive-membrane.html.
[172] Danish Power Systems. High Temperature PEM Fuel Cells n.d. https://daposy.com/fuel-cells.
[173] Abdul Rasheed RK, Liao Q, Caizhi Z, Chan SH. A review on modelling of high temperature proton exchange membrane fuel cells (HT-PEMFCs). Int J Hydrogen Energy 2017;42:3142–65. https://doi.org/10.1016/j.ijhydene.2016.10.078.
[174] Moçotéguy P, Ludwig B, Scholta J, Barrera R, Ginocchio S. Long term testing in continuous mode of HT-PEMFC based H3PO 4/PBI celtec-PMEAs for μ-CHP applications. Fuel Cell 2009;9:325–48. https://doi.org/10.1002/fuce.200800134.
[175] Mocotéguy P, Ludwig B, Scholta J, Nedellec Y, Jones DJ, Rozière J. Long-term testing in dynamic mode of HT-PEMFC H3PO 4/PBI celtec-P based membrane electrode assemblies for micro-CHP applications. Fuel Cell 2010;10:299–311. https://doi.org/10.1002/fuce.200900153.
[176] Borup RL, Davey JR, Garzon FH, Wood DL, Inbody MA. PEM fuel cell electrocatalyst durability measurements. J Power Sources 2006;163:76–81. https://doi.org/10.1016/j.jpowsour.2006.03.009.
[177] Kannan A, Kabza A, Scholta J. Long term testing of start-stop cycles on high temperature PEM fuel cell stack. J Power Sources 2015;277:312–6. https://doi.org/10.1016/j.jpowsour.2014.11.115.
[178] Kannan A, Kaczerowski J, Kabza A, Scholta J. Operation strategies based on carbon corrosion and lifetime investigations for high temperature polymer electrolyte membrane fuel cell stacks. Fuel Cell 2018;18:287–98. https://doi.org/10.1002/fuce.201700096.
[179] Kurtz M, Wilmer H, Genger T, Hinrichsen O, Muhler M. Deactivation of supported copper catalysts for methanol synthesis. Catal Lett 2003;86:77–80. https://doi.org/10.1023/A:1022663125977.
[180] Baydir E, Aras Ö. The role of CO adsorption and CuO formation on the catalyst deactivation during the long-term performance evaluation of methanol steam reforming process for hydrogen production: Comparison of sono-coprecipitation and spray pyrolysis method. Int J Hydrogen Energy 2022;47:38594–608. https://doi.org/10.1016/J.IJHYDENE.2022.09.031.
[181] Lindström B, Pettersson LJ. Deactivation of copper-based catalysts for fuel cell applications. Catal Lett 2001;74.
[182] Twigg Mv, Spencer MS. Deactivation of copper metal catalysts for methanol decomposition, methanol steam reforming and methanol synthesis. Top Catal 2003;22:191–203. https://doi.org/10.1023/A:1023567718303. 3 2003;22.
[183] Park JE, Yim SD, Kim CS, Park ED. Steam reforming of methanol over Cu/ZnO/ZrO2/Al 2O3 catalyst. Int J Hydrogen Energy 2014;39:11517–27. https://doi.org/10.1016/j.ijhydene.2014.05.130.
[184] Serenergy. Fuel cell units n.d. https://serene.advent.energy/units/.
[185] Nasri M, Dickinson D. Thermal management of fuel cell-driven vehicles using HT-PEM and hydrogen storage. In: 2014 ninth international conference on ecological vehicles and renewable energies. EVER; 2014. p. 1–6. https://doi.org/10.1109/EVER.2014.6844107.
[186] Aghbashlo M, Rosen MA. Exergoeconoenvironmental analysis as a new concept for developing thermodynamically, economically, and environmentally sound energy conversion systems. J Clean Prod 2018;187:190–204. https://doi.org/10.1016/J.JCLEPRO.2018.03.214.
[187] Forootan MM, Larki I, Zahedi R, Ahmadi A. Machine learning and deep learning in energy systems: a review. Sustainability 2022;14:4832. https://doi.org/10.3390/SU14084832. 2022;14:4832.
[188] Strušnik D, Avsec J. Exergoeconomic machine-learning method of integrating a thermochemical Cu–Cl cycle in a multigeneration combined cycle gas turbine for hydrogen production. Int J Hydrogen Energy 2022;47:17121–49. https://doi.org/10.1016/J.IJHYDENE.2022.03.230.
[189] James BD, Desantis DA. Manufacturing cost and installed price analysis of stationary fuel cell systems. 2015.
[190] EU. Renewable energy targets n.d. https://energy.ec.europa.eu/topics/renewable-energy/renewable-energy-directive-targets-and-rules/renewable-energy-targets_en.
[191] Cui X, Kær SK, Nielsen MP. Energy analysis and surrogate modeling for the green methanol production under dynamic operating conditions. Fuel 2022;307:121924. https://doi.org/10.1016/j.fuel.2021.121924.